TECHNICAL EVALUATION REPORT

MONTE CARLO UNCERTAINTY ANALYSIS OF AEROSOL BEHAVIOR IN THE AP600 REACTOR CONTAINMENT UNDER CONDITIONS OF A SPECIFIC DESIGN - BASIS ACCIDENT PART 1

D. A. POWERS
Sandia National Laboratories
Albuquerque, NM 87185

June 1995

9607260129 960717
PDR ADOCK 05200003
A PDR

ABSTRACT

A Monte Carlo uncertainty analysis of aerosol behavior in the AP600 reactor containment during a hypothetical 3BE accident is described. The analysis used fixed (not uncertain) boundary conditions for pressure, containment atmosphere temperature, mole fraction stream in the atmosphere, rate of steam condensation from the atmosphere, and rate of heat removal from the atmosphere. The NUREG-1465 radionuclide source terms to the containment were also treated as certain inputs to the analysis. Uncertainties considered in the Monte Carlo analysis are nonradioactive aerosol mass, aerosol properties, thermal and momentum accommodation coefficients, primary aerosol particle size and coefficients in correlations for turbulent natural convection processes.

Uncertainty distributions for decontamination factors and decontamination coefficients were constructed using nonparametric order statistics. Results are compared to "point" values calculated by others for the same problem using the NAUAHYGROS model. It is found that effective decontamination coefficients calculated in the Monte Carlo uncertainty analysis are smaller than average decontamination coefficients calculated with the NAUAHYGROS model. Results of the NAUAHYGROS calculations exceed the 90 percentile of uncertainty distributions developed in the Monte Carlo uncertainty analysis. The discrepancy may be due to a large nonradioactive aerosol source term used in the NAUAHYGROS calculations.

TABLE OF CONTENTS

LIST OF FIGURES

LIST OF TABLES (Concluded)

LIST OF TABLES

I. STATEMENT OF THE ISSUE

This document describes a Monte Carlo uncertainty analysis of aerosol behavior in the containment of the AP600 nuclear power plant under the conditions of a particular, hypothetical, design-basis accident. This analysis was done to assess the conservatism of analyses of aerosol behavior for design certification of the AP600 advanced light water reactor.

A. BACKGROUND

Modern analyses of radionuclide releases to the atmosphere of containments of nuclear power reactors recognize that much of radioactive material discharged to the containment atmosphere will be in the form of aerosol particles. This recognition has been codified in the Severe Reactor Accident Source Term recently prepared by the U.S. Nuclear Regulatory Commission [1]. The radionuclide releases to the containment (the source term) specified in this document is often called the "NUREG-1465 source term." The NUREG-1465 source term specifies releases of seven classes of radionuclides in addition to noble gases that pass into the containment atmosphere. With the exception of the noble gases and a small fraction of the iodine, the radioactive materials are considered to be aerosol particles. This description of the radionuclide releases to the containment atmosphere can be contrasted with an older source term description (the TID-14844 source term) that emphasized releases of the noble gases and iodine in gaseous form [2].

Radionuclides suspended in the reactor containment atmosphere can leak from the plant. Leakage of radionuclides is mitigated by natural and engineered processes that remove radionuclides from the atmosphere. Under design basis accident conditions, existing pressurized water reactors have containment sprays that can rapidly scrub aerosol particles from the containment atmosphere [3]. Such active, engineered systems for decontaminating the containment atmosphere have not been incorporated into the AP600 design. Instead, natural aerosol deposition processes are expected to mitigate sufficiently the amount of radioactive material suspended in the AP600 containment atmosphere.

There are, indeed, many natural processes that will cause aerosol particles to grow and to deposit from a containment atmosphere [4]. These natural processes can take longer to decontaminate the containment atmosphere than do engineered safety systems such as containment sprays. Preliminary analyses of the decontamination of the AP600 containment by natural aerosol processes were done using models and boundary conditions better suited for the analysis of aerosol behavior during accidents in existing light water reactors [4]. These preliminary analyses suggested that decontamination of the AP600 containment atmosphere by natural aerosol processes would, indeed, be slow. A safety concern arose that there would be prolonged periods in an accident with relatively high concentrations of radionuclides in the containment that could leak from the plant.

The AP600 reactor containment is, however, quite different than containments of existing pressurized water reactors. External cooling of the containment boundary provides continuing driving forces for the removal of aerosol particles by phoretic processes (diffusiophoresis and thermophoresis). Though these aerosol removal processes are expected to contribute to aerosol decontamination during accidents in existing light water reactors, they become less significant as the containments heat. Analyses of aerosol removal prepared for the design certification of the AP600 reactor using the NAUAHYGROS computer code indicate significantly more rapid ($\sim 5x$) aerosol removal than is predicted with models designed for analysis of accidents in existing light water reactors.

There are many uncertainties that may affect predictions of aerosol behavior under reactor accident conditions. There are uncertainties about the boundary conditions (containment atmosphere temperature, pressure, composition, etc.). There are also phenomenological uncertainties about the properties and behaviors of aerosols. These phenomenological uncertainties were treated differently in the NAUAHYGROS calculations than in the model used for preliminary analysis of aerosol behavior in the AP600 containment. Discrepancies in the results of the two analyses might, then, be the result of different treatments of boundary conditions or different treatments of uncertain phenomena.

B. THE ISSUE

To identify the causes of discrepancies between predicted rates of containment decontamination by natural aerosol processes obtained with the NAUAHYGROS code and the preliminary calculations based on existing light water reactors, analyses have been done for the same hypothesized reactor accident using the geometry of the AP600 reactor and the boundary conditions for a particular accident. The results reported here are for a Monte Carlo uncertainty analysis of aerosol behavior in which uncertainties in the containment geometry and uncertainties in the boundary conditions have been eliminated. Phenomenological uncertainties concerning the properties and behavior of aerosol particles released to the containment atmosphere have been considered. Uncertainty distributions for the decontamination factors and the decontamination coefficients derived from results of the Monte Carlo analyses can be compared to point values for these quantities estimated with the NAUAHYGROS code. The comparison provides an indication of the conservatism inherent in the NAUAHYGROS results with respect to phenomenological uncertainties.

II. THE APPROACH

A. OVERVIEW

To resolve the issue described in Section I, a Monte Carlo uncertainty analysis similar in nature to uncertainty analyses of other aerosol issues described elsewhere [3-6] was undertaken for aerosol behavior in the AP600 reactor containment. This uncertainty analysis paralleled closely an uncertainty analysis of containment decontamination by natural aerosol processes in existing light water reactors [4]. The analyses of natural aerosol processes in

existing light water reactor containments explicitly considered uncertainties in predicted aerosol removal caused by uncertainties in accident boundary conditions (such as containment atmosphere temperature, pressure, composition and thermal hydraulics), aerosol properties (such as particle size, shape factors, etc.) and aerosol processes (collision efficiencies, accommodation, slip, etc.). Uncertainties in accident boundary conditions for existing light water reactors had been based on results of analyses of a variety of severe (beyond design basis) accidents done with the Source Term Code Package (7-11). These boundary condition uncertainties were eliminated in the Monte Carlo analysis of aerosol behavior in the AP600 reactor containment by using boundary conditions obtained using the MAAP code to predict conditions for a specific accident—the 3BE accident involving a break in an 8" direct vessel injection line. Uncertainty distributions found here reflect uncertainties in aerosol processes, aerosol properties and the source nonradioactive aerosol source term to the reactor containment atmosphere.

Uncertainties considered in the Monte Carlo analysis are discussed further in Sections II-C and II-D of this report and in greater detail in Reference 4. Three possible sources of uncertainty in the predicted behavior of aerosol in the reactor containment are implicitly omitted along with explicit omission of the boundary condition uncertainties. It is assumed that the containment atmosphere is thoroughly mixed and that stagnant or compositional stratified layers do not develop. This could be a significant omission since, as discussed below, diffusiophoresis is found to be a dominant mechanism for aerosol removal for the accident considered here. Stagnation could, of course, arrest diffusiophoresis. It is also assumed that electrostatic charging effects on both the agglomeration of aerosol particles and the deposition of aerosol particles can be neglected. Though definitive analyses have not been done, it is thought that neglect of the electrostatic charging effects is a conservative approximation [4]. That is, electrostatic effects are thought to enhance aerosol agglomeration and deposition.

Finally, it is assumed that particles do not grow by water absorption into hygroscopic materials. Though some chemical species suggested to be present in aerosols produced by reactor accidents are quite hygroscopic (CsOH and CsI, are examples), it is not established that such materials are actually present. Hygroscopic chemical forms are, in general, quite chemically reactive and can be expected to form species of low hygroscopicity given sufficient time. Furthermore, it is not apparent that hygroscopic materials coagglomerated with large amounts of nonhygroscopic materials will cause significant aerosol particle growth by water adsorption. In any event, neglect of particle growth by water adsorption is a conservative approximation. (Note, however that it is assumed water will condense in concave pores within particles—see section II-D.5)

Independent analyses of aerosol behavior in the AP600 containment were done by others [12] using the NAUAHYGROS computer code [13]. These analyses yielded "point" values of the aerosol decontamination coefficients since the effects of uncertainties on the predictions of aerosol behavior were not explicitly considered. Comparison of these point values with the uncertainty distributions found in the Monte Carlo calculations reported here can be used to

estimate the conservatism inherent in the point values with respect to uncertainties in aerosol properties, aerosol processes and the source term to the containment. This comparison is discussed further in Section III of this report.

B. CONTAINMENT GEOMETRY AND ACCIDENT BOUNDARY CONDITIONS

Containment geometry data were obtained from the Westinghouse Electric Corporation [12]. Geometry data used in the Monte Carlo analyses are:

Containment Volume:	4.7927×10^{10} cm^3
Upward-facing Area:	1.848×10^{7} cm^2
Vertical Area:	7.04×10^{7} cm^2
Containment cylinder equivalent height:	4311 cm.

These geometry data for the AP600 containment were used in place of the correlations of containment geometry with reactor power used in the analyses of natural aerosol processes in the containments of existing light water reactor [4]. Uncertainties ascribed to the geometry correlations, then, do not arise in the analyses reported here.

Predictions of the containment boundary conditions by the MAAP code for the hypothetical 3BE accident were obtained from the Westinghouse Electric Corporation [12]. Boundary conditions used in the Monte Carlo analyses are:

- containment pressure,
- containment atmospheric temperature,
- mole fraction steam in the containment atmosphere,
- steam condensation rate, and
- rate of heat removal from the containment atmosphere.

These boundary conditions are shown as functions of time in Figure 1 to 5. Note that the origins in these figures correspond to a time 1.6 hours after initiation of the accident when the water level has fallen to the top of the active fuel in the reactor vessel [12]. It has been assumed here that no significant release of radioactivity in aerosol to the containment atmosphere would occur until the coolant level fell below the top of the active fuel. That is, radioactivity in the coolant that might be dispersed as aerosols in the containment prior to the coolant level falling to the top of the active fuel has been neglected.

The boundary condition data were provided as tabulations. These tabular inputs to the Monte Carlo analyses are reproduced in Appendix A. Linear interpolation among the tabulated values was used in the Monte Carlo analyses. Test calculations indicated no great differences in the calculated behavior of the aerosol were obtained when the boundary conditions were used as piece-wise constants.

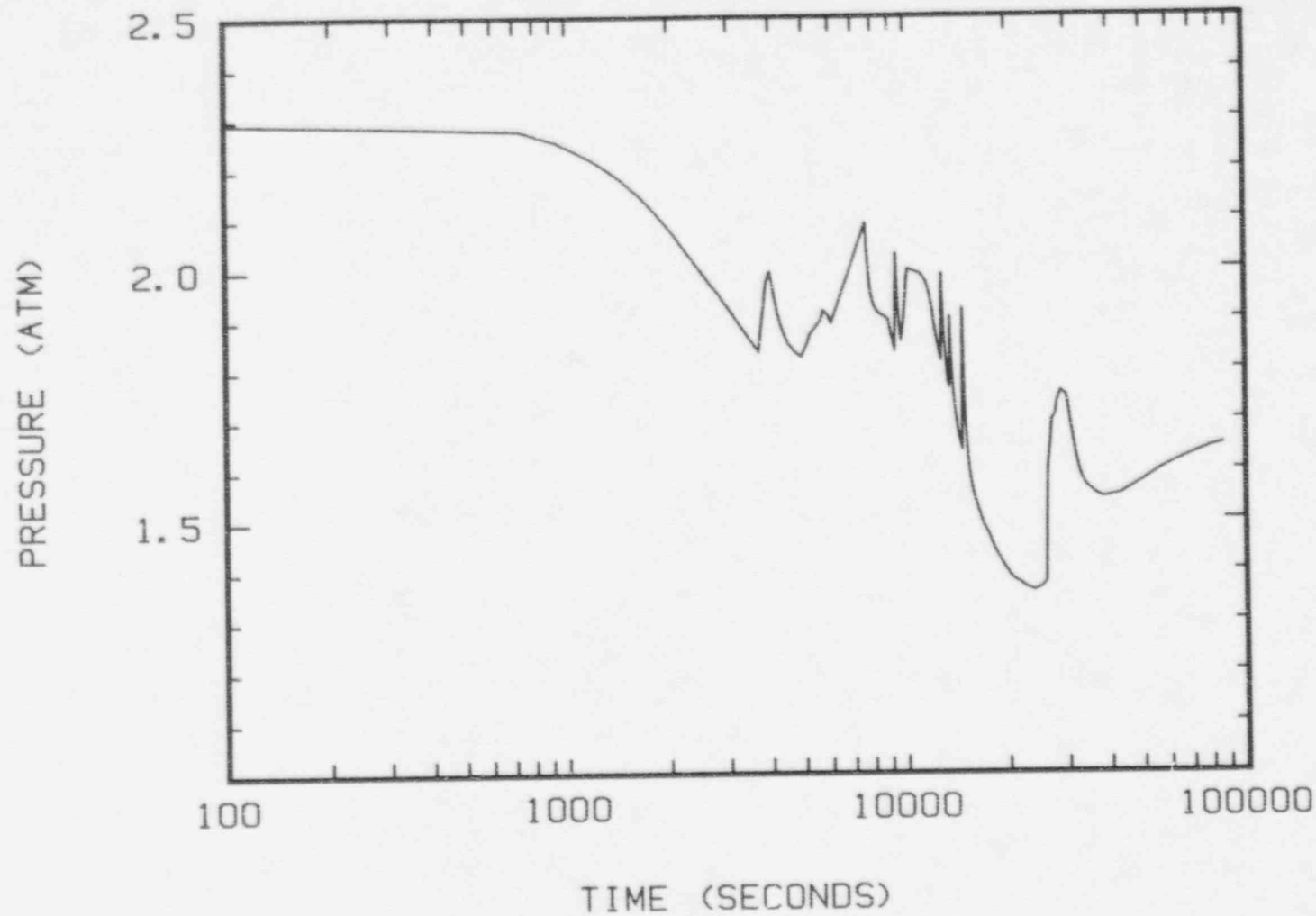

Figure 1. Containment Pressure as a Function of Time.

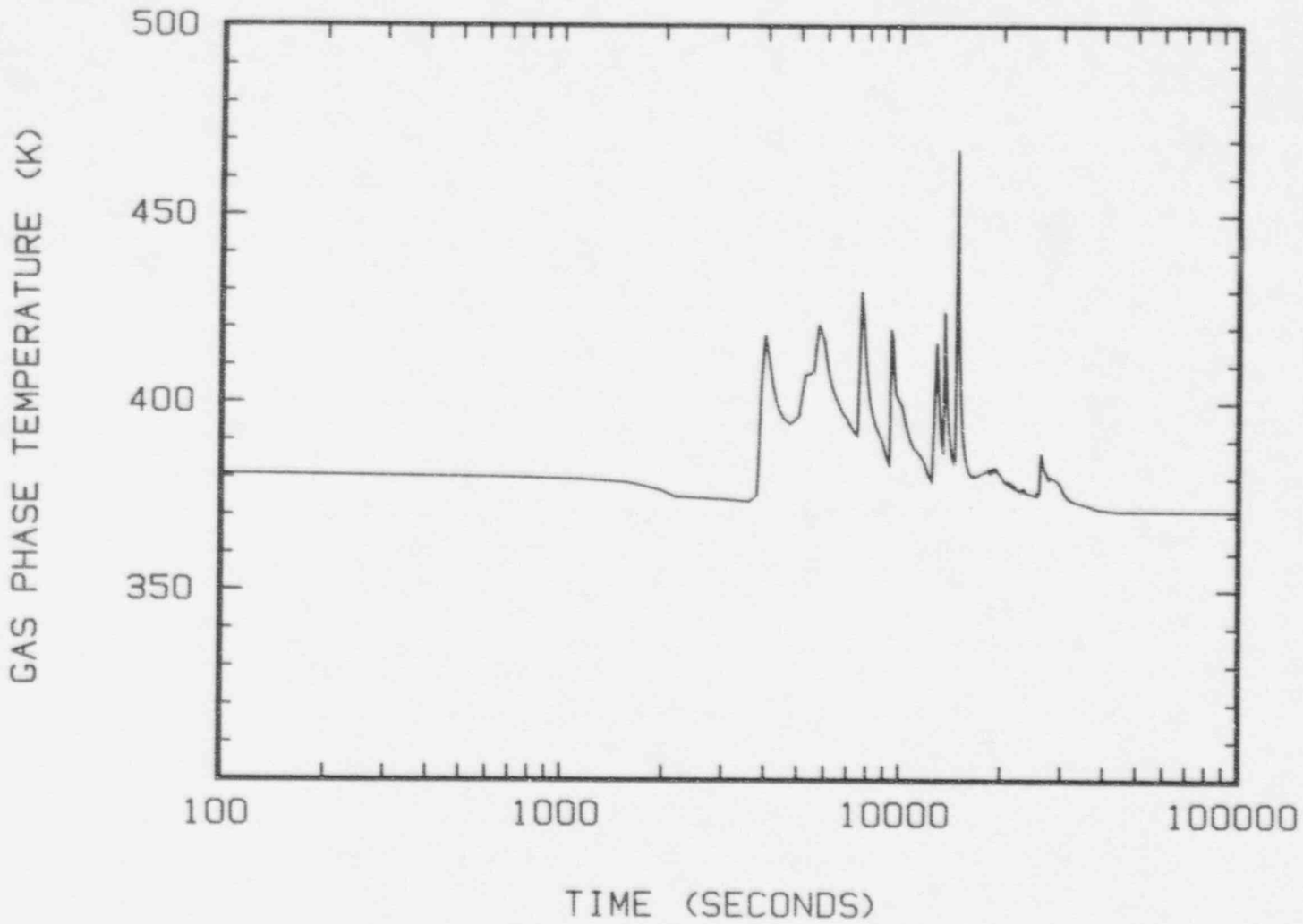

Figure 2. Containment Atmosp' ere Temperature as a Function of Time.

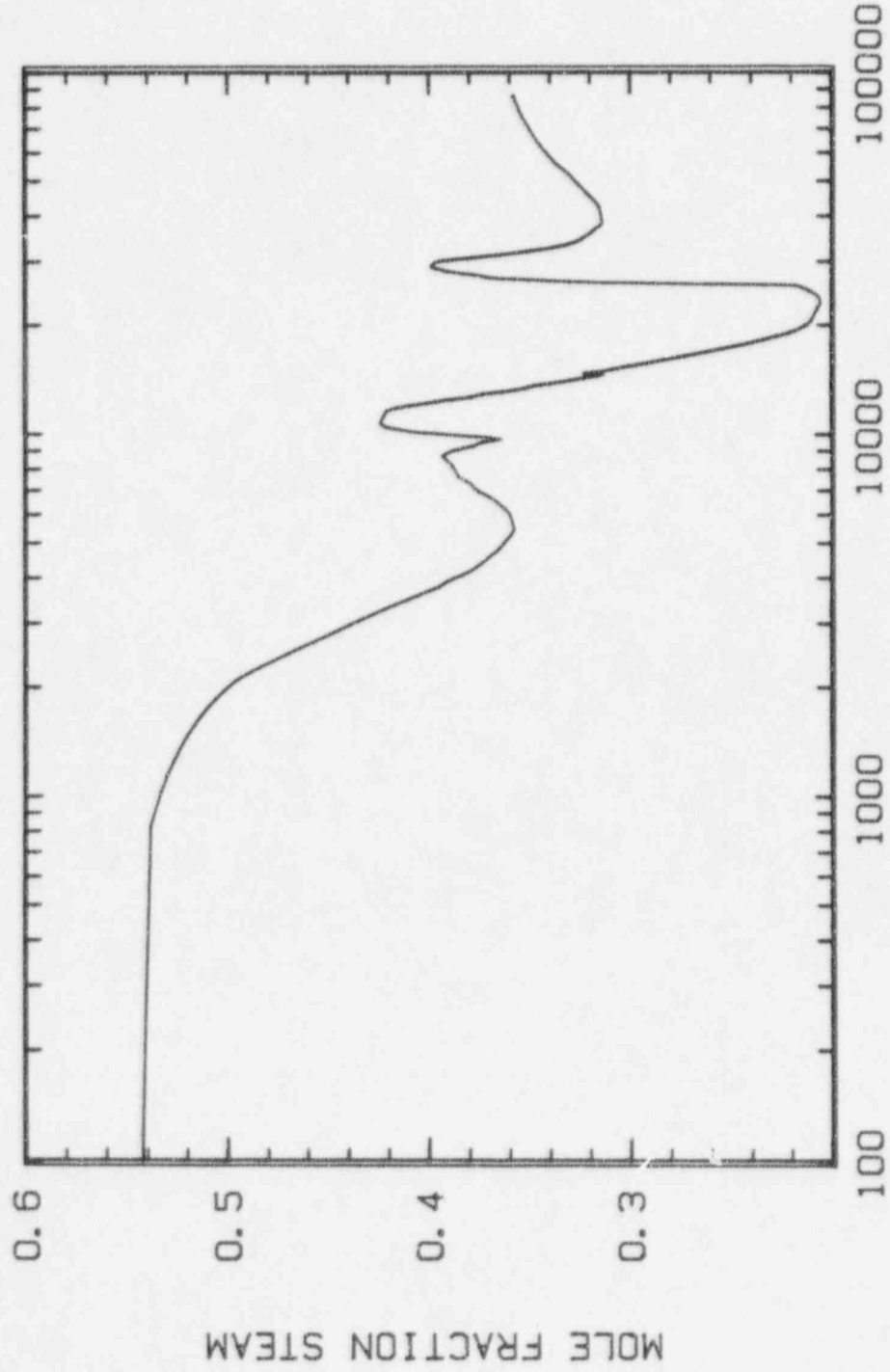

Figure 3. Mole Fraction Steam in the Containment Atmosphere as a Function of Time.

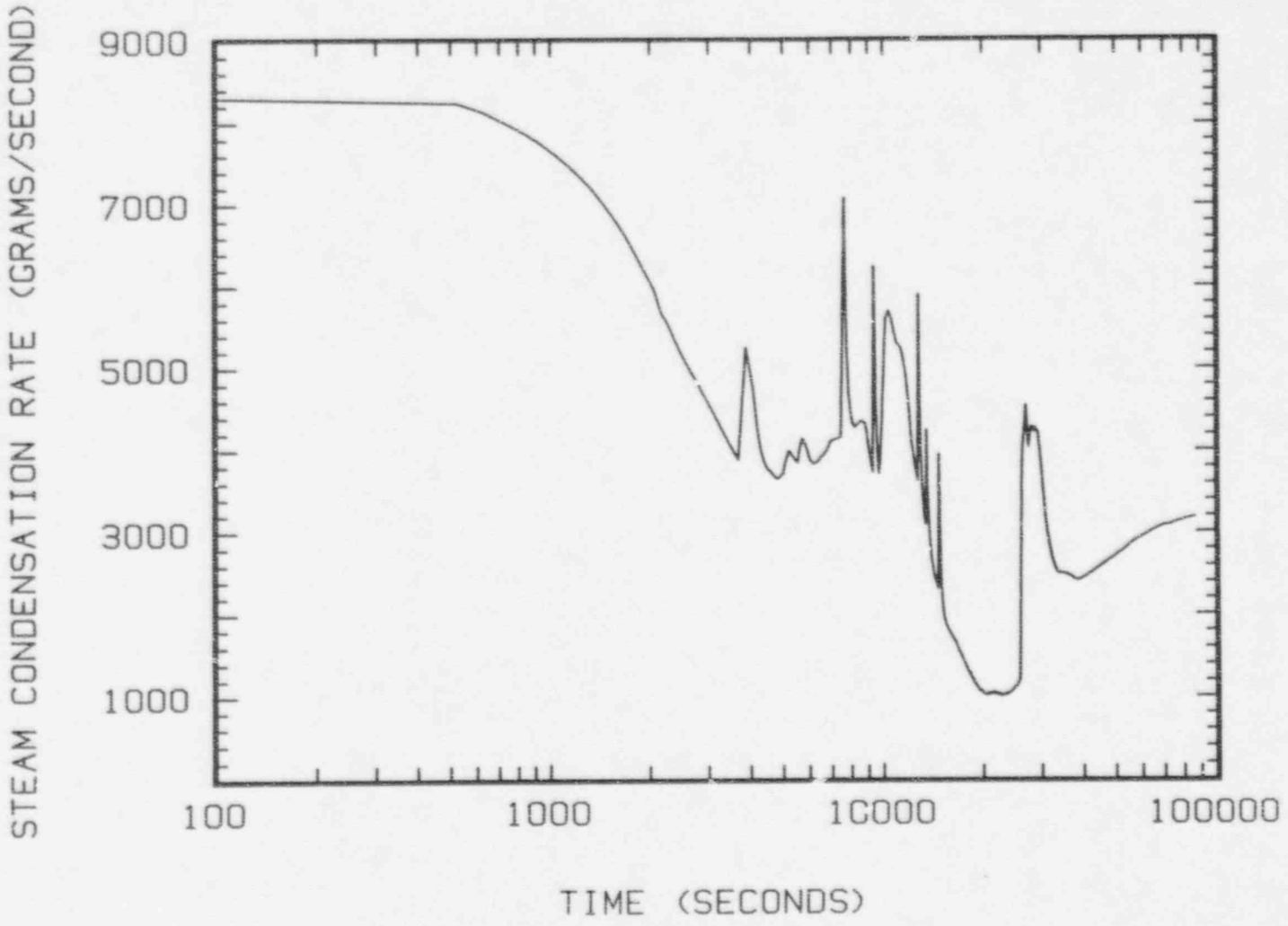

Figure 4. Rate of Steam Condensation From the Containment Atmosphere as a Function of Time.

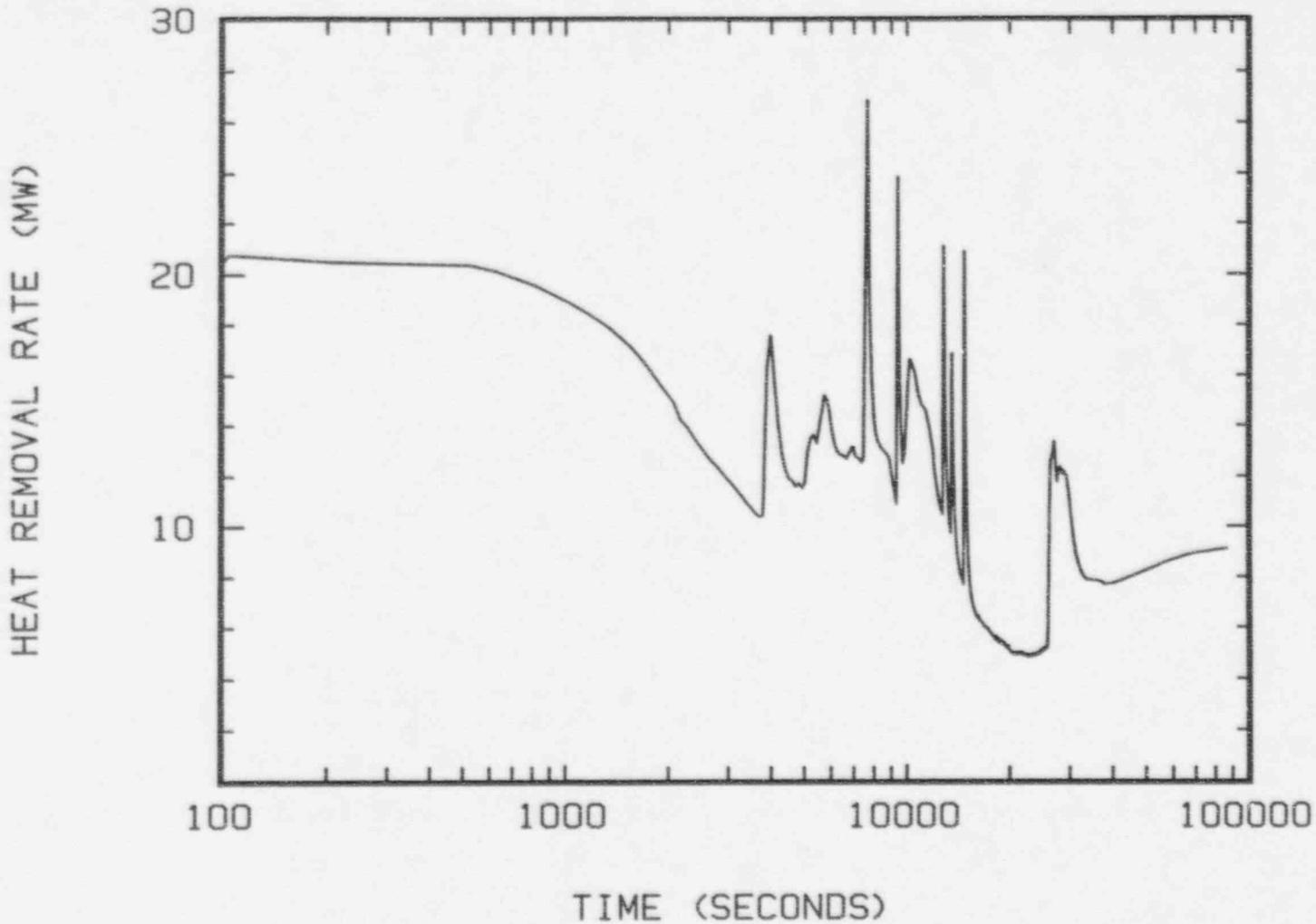

Figure 5. Rate of Heat Removal From the Containment Atmosphere as a Function of Time.

Boundary conditions vary smoothly with time throughout the duration of gap release (0 to 1800 seconds) and during the early portion of the in-vessel release (1800 to 6480 seconds). After about 3500 seconds, boundary conditions are marked by a series of sharp spikes in temperature, pressure and steam mole fraction. These spikes must reflect fairly dramatic events taking place during core degradation such as melt relocation from the core region into the lower plenum of the reactor vessel. Spikes also occur in the rates of steam condensation and heat removal from the containment atmosphere. Abrupt increases in the calculated rates of aerosol removal can be expected at the times of these spikes in the containment boundary conditions. No consideration of the uncertainties in the existence, magnitude or timing of these spikes was undertaken here. Calculations were done for the Monte Carlo uncertainty analysis in such a way that the effects of these transient excursions on natural aerosol processes were reflected in the results. In the preliminary analyses of aerosol behavior in the AP600 containment, no transient excursions in boundary conditions had been considered.

A broad minimum in the rate of steam condensation occurs over the interval of about 19000 to 27000 seconds. After 28000 seconds, the steam condensation rate rises to a plateau. Corresponding changes in the other boundary conditions occur at these times. These changes can also be expected to affect the rates of aerosol removal from the containment atmosphere by phoretic processes (diffusiophoresis and thermophoresis). The causes of these changes in the boundary conditions were not investigated as part of this work despite the effects they could be expected to have on aerosol behavior.

The computer code used for the Monte Carlo uncertainty analysis internally calculates the difference between the bulk atmosphere temperature and the mean structural surface temperature [4]. This temperature difference, ΔT, is calculated from the following equations [4, 14].

$$\frac{\dot{Q}}{A} = h^* \Delta T + \Delta H_{fg} \dot{m}(H_2O)$$

where

$\dot{Q}$ = rate of heat removal from the containment atmosphere

A = surface area

ΔH_{fg} = latent heat of steam condensation

$\dot{m}(H_2O)$ = mass rate of steam condensation, and

h^* = heat transfer coefficient.

The heat transfer coefficient was calculated iteratively from the equations:

$$k_m^* = \frac{mR(2T - \Delta T)}{x(H_2O)P - P_{sat}(T - \Delta T)}$$

$$k_m = k_m^* / C_o$$

$$C_o = \ln(1 + \underline{R}) / \underline{R}$$

$$\underline{R} = \frac{P_{sat}(T - \Delta T) / P - x(H_2O)}{1 - P_{sat}(T - \Delta T) / P}$$

$$k_m = \frac{\varepsilon(Sh)}{Re^{1/4}\ Sc^{2/3}}$$

$$Re = P_g \Gamma \delta / \mu_g$$

Sc = Schmidt number of gas

$$\delta = \frac{0.565\ L}{Gr^{0.1}\ Pr^{8/15}} \frac{1}{\left(1 + 0.494\ Pr^{2/3}\right)^{0.1}}$$

$$\Gamma = \frac{1.185\left(\frac{\mu_g}{\rho_g L}\right) Gr^{1/2}}{\left(1 + 0.494\ Pr^{2/3}\right)^{1/2}}$$

$$Gr = \frac{g}{T} \frac{\Delta T L^3}{\mu_g^2} \rho_g^2$$

Pr = Prandtl number

$$h = \frac{k_g(th)\,\varepsilon\,(Nu)\,Gr^{0.4}\,Pr^{7/15}}{L\left(1 + 0.494\,Pr^{2/3}\right)^{0.4}}$$

and ε(Sh) and ε(Nu) are uncertain dimensionless coefficients uniformly distributed over the ranges 0.0094 to 0.0376 and 0.0148 to 0.059, respectively.

C. SOURCE TERM

1. Radionuclides

The radionuclide source term to the reactor containment atmosphere for the Monte Carlo uncertainty analysis was taken to be certain and to be that specified in NUREG-1465 for the gap release and the in-vessel release phases of a pressurized water reactor accident. This source term is shown in Table 1. Releases specified in NUREG-1465 for the ex-vessel and the late in-vessel phases of a severe reactor accident were not considered for this work with a design-basis accident.

Table 1. NUREG-1465 Pressurized Water Reactor Accident Source Term to the Containment

	Fraction of Initial Core Inventory Released to the Containment During the	
Element	Gap Release (0-1800 s)	In-Vessel Release (1800-6480 s)
I	0.05	0.35
Cs	0.05	0.25
Te	0	0.15
Sr	0	0.03
Ba	0	0.04
Ru	0	0.008
Ce	0	0.01
La	0	0.002

The NUREG-1465 source term is specified in terms of the fractions of initial core inventories of radionuclides released at constant rates over various phases of an accident. To convert these release specifications to radioactive aerosol mass, it is necessary to know the core inventories of radionuclides. For this comparison work, however, the elemental releases used in the Monte Carlo analyses were chosen to match the elemental releases specified by the

source term adopted for calculations of the hypothesized AP600 accident with the NAUAHYGROS model. The source terms of radionuclides for the uncertainty analyses, then are:

	Release Rate (grams element/s)	
Element	Gap Release (0-1800 s)	In-Vessel Release (1800-6480 s)
Cs	6.11065	10.3415
I	0.49998	1.3461
Te	0	0.405983
Ba	0	0.51284
Sr	0	0.30341
Ce	0	0.022435
La	0	0.00414526
Ru	0	0.101496

The chemical forms that will be adopted by radionuclides released to a reactor containment atmosphere are quite uncertain. For the Monte Carlo uncertainty analyses, the elemental release masses were multiplied by a factor to account for possible oxidation and hydration of the elements. These multiplicative factors were treated as uncertainties in the Monte Carlo analysis as described in section II-D. Specific chemical forms of the radioactive elements were adopted for the analyses done with NAUAHYGROS [12]. The implied mass factors for the NAUAHYGROS source term are shown in Table 2.

2. Nonradioactive Aerosol Mass

Radioactive materials are not the only aerosol released into the containment atmosphere during an accident. Nonradioactive materials that form aerosols are also generated in an accident. These nonradioactive aerosols will agglomerate with radioactive aerosols and enhance the removal of both classes of aerosol. Unfortunately, there is a poor understanding of the releases of nonradioactive aerosol materials during reactor accidents. The NAUAHYGROS point estimates were obtained assuming that the ratio of nonradioactive aerosol mass to radioactive aerosol mass was 0 throughout the gap release phase and about 3.6245 during the in-vessel release phase of the 3BE accident. The releases of nonradioactive aerosol mass were taken to be uncertain in the Monte Carlo uncertainty analyses. Furthermore, the ratios of nonradioactive aerosol mass to radioactive aerosol mass were taken to be different during the gap release and the in-vessel release phases of the accident. The treatment of these uncertainties is described in Section II-D. In general, the ratios of the nonradioactive mass to radionuclide mass used in the Monte Carlo analyses are smaller than the value of 3.6245 used for the NAUAHYGROS calculations. Some compensation for this discrepancy is provided by the treatment of radionuclide chemical form in the Monte Carlo analyses.

Table 2. Uncertain Quantities Considered in the Monte Carlo Uncertainty Analysis

Quantity	Plausible Range of Values	Distribution of Values	Values used in the NAUAHYGROS Calculations
Mass multiplier to account for the chemical forms of radionuclides released to the containment			
I	1.0 to 1.38	uniform	1.0
Cs	1.05 to 1.22	uniform	1.12
Te	1.0 to 1.25	uniform	1.0
Sr,Ba	1.18 to 1.67	uniform	1.18
Ru	1.0 to 1.47	uniform	1.0
Ce	1.17 to 1.22	uniform	1.22
La	1.11 to 1.17	uniform	1.17
Nonradioactive aerosol mass to radioactive aerosol mass during:			
gap release	0.01 to 1.0	log-uniform	0
in-vessel release	0.5 to 2.0	uniform	3.6245
aerosol material density during gap release (g/cm^3)	2.8 to 4.5	uniform	3
Aerosol material density during in-vessel release (g/cm^3)	3.25 to 10.96	log-uniform	
Material thermal conductivity of aerosol released during:			
- the gap release (cal/cm-s-K)	0.023 to 0.0022	log-uniform	Value for water
- the in-vessel release (cal/cm-s-K)	0.1 to $3x10^{-4}$	log-uniform	Value for water

Table 2. Uncertain Quantities Considered in the Monte Carlo Uncertainty Analysis (Continued)

Quantity	Plausible Range of Values	Distribution of Values	Values used in the NAUAHYGROS Calculations
Coefficient to describe contact resistance	10^{-3} to 0.5	log-uniform	NA
Coefficient in the correlation of the heat transfer coefficient	0.0148 to 0.059	uniform	NA
Coefficient in the correlation of the mass transport coefficient	0.0084 to 0.0376	uniform	NA
Parameter relating the natural convection mass transport length scale to containment height	0.1 to 1.0	log-uniform	NA
Fractal dimension of particle agglomerates	1.5 to 2.24	uniform	NA
Diameter of primary aerosol particles (μm)	0.02 to 0.2	log-uniform	NA
Coefficient in the expression for collision efficiency	0.1 to 1.0	log-uniform	1/3
Coefficient in the expression for momentum accommodation coefficient	0.0 to 0.6	uniform	implicitly fixed
Coefficient in the expression for the thermal accommodation coefficient	0.0 to 0.6	uniform	implicitly fixed
ξ(s), term to account for the gas/surface potential in the Cs parameter for the model of the thermophoretic deposition	0.35 to 0.383	uniform	NA

Table 3. Uncertain Quantities Considered in the Monte Carlo Uncertainty Analysis (Concluded)

Quantity	Plausible Range of Values	Distribution of Values	Values used in the NAUAHYGROS Calculations
$\xi(t)$, term to account for the gas/surface potential in the temperature jump parameter for the model of thermophoretic deposition	1.263 to 1.296	uniform	NA
$\xi(m)$, term to account for the gas/surface potential in the momentum jump parameter for the model of thermophoretic deposition	0.996 to 1.020	uniform	NA
(σ_{12}), parameter to select among models for the diffusiophoretic scattering kernal	0 to 1.0	uniform	0
$\xi(u^*)$, parameter in the definition of friction velocity	0.1464 to 0.5370	uniform	NA

D. UNCERTAINTIES CONSIDERED IN THE MONTE CARLO ANALYSIS

Uncertainties considered in the Monte Carlo uncertainty analysis of aerosol behavior in the AP600 reactor containment are listed in Table 2. Each of the uncertainties is characterized by a parameter with a plausible range of values and a distribution of values within this range. In general, uniform and log-uniform distributions have been used for the uncertainty analyses reported here. In the Monte Carlo uncertainty analyses, values of the uncertain parameters are randomly selected in accordance with their respective subjective probability distributions. Calculations of aerosol behavior are carried out, the results accumulated, and a new set of parametric values is selected. The process is repeated and results are accumulated until there is a 99 percent confidence that 95 percent of the range of values of the results has been sampled. The accumulated set of results is analyzed using nonparametric, order statistics to define uncertainty distributions for the calculated quantities. Additional information on the construction of uncertainty distributions from the accumulated results of Monte Carlo analyses can be found in Appendix A of Reference 5.

Each of the phenomenological uncertainties considered in the Monte Carlo uncertainty analysis of aerosol behavior in the AP600 reactor containment is briefly discussed in the subsections that follow. Synoptic justifications for the plausible ranges of parametric values are presented. Additional, more detailed information including a description of the rationale for selecting the high entropy distributions for values within the respective ranges can be found in Reference 4.

1. Mass Multiplier to Account for the Chemical Form of Radionuclides

The NUREG-1465 source term specifies elemental releases. In general, radionuclides will not all be in elemental form when they reach the containment. The exact chemical form adopted by the radionuclides is, however, not well known. It is often suggested for instance that cesium is released into the reactor containment as CsOH. But, CsOH is quite a reactive species and may be easily converted to Cs_2CO_3 by reaction with carbon dioxide in the containment atmosphere, or it might be converted to $CsBO_2$ by reaction with boric acid vaporized from the reactor coolant. Similarly, iodine is often thought to be present as CsI. It can, however, be further oxidized to $CsIO_3$ or it can react with ozone produced by radiolysis of the atmosphere to form IO_{2+x} where x may be between 0 and 1. On the other hand iodine may be present in the containment atmosphere as AgI which exhibits none of the hygroscopic properties of CsI.

The additional aerosol mass created by radionuclide reactions with species such as carbon dioxide, oxygen or steam that would otherwise be gaseous in the containment will affect the removal of aerosols from the atmosphere. This additional mass must, then, be considered. The additional mass is accounted here by multiplying the aerosol mass of each radionuclide by a factor. The factor is uncertain because the chemical forms of the radionuclides under conditions that prevail in the reactor containment are not known. Plausible ranges for the multiplicative factors were selected by considering limiting chemical forms of the radionuclides:

Element	Plausible Chemical Forms	Plausible Range of Multiplicative Mass Factors
I	I^- ; IO_3	1.0 to 1.38
Cs	$CsO_{1/2}$; $Cs(CO_3)_{1/2}$	1.05 to 1.22
Te	Te ; TeO_2	1.0 to 1.25
Sr	SrO; $SrCO_3$	1.18 to 1.67
Ru	Ru ; RuO_3	1.0 to 1.47
Ce	$CeO_{1.5}$; CeO_2	1.17 to 1.22
La	LaO; $LaO_{1.5}$	1.11 to 1.17

The NAUAHYGROS calculations considered specific chemical forms for the radionuclides. The multiplicative mass factors implied by these assumed forms are compared in Table 2 to the uncertainty ranges for these factors used in the Monte Carlo uncertainty analysis. In general, the implied multiplicative factors used in the NAUAHYGROS calculations fall within the uncertainty ranges used for the Monte Carlo analyses.

2. Nonradioactive Aerosol Production

Reactor accident source terms focus on the release of radionuclides to the reactor of radionuclides to the reactor containment. From the perspective of containment decontamination by natural aerosol processes, the nonradioactive aerosol mass in the containment atmosphere is just as important as the radioactive aerosol mass. Accurate assessments of aerosol behavior in the containment atmosphere must take into account the nonradioactive aerosol mass. Unfortunately, much less is known about the releases of nonradioactive aerosols to the containment atmosphere than is known about releases of radionuclides to the containment.

It is certainly recognized that there are sources of nonradioactive aerosol that are potentially large. In the case of pressurized water reactors, boric acid vaporized from the coolant or cadmium from the reactor control rods could be massive sources of aerosol. Tin from the fuel cladding, uranium oxides from the fuel, or constituents of steel from the reactor intervals are other potential sources of nonradioactive aerosol mass. At the elevated temperatures of reactor core degradation these materials could vaporize. As the vapors emerge from the core region into cooler portions of the reactor coolant system and, eventually, into the containment, the vapors can condense to contribute to the aerosol in containment. Nonradioactive aerosols will coagulate with radioactive particles to create indistinguishable airborne particles. The effect of the nonradioactive aerosol is to increase the airborne mass and thereby increase the driving forces for aerosol particle growth. It is generally true that large aerosol particles are more rapidly removed from the containment atmosphere than are smaller (but not very small <0.1 μm) particles. Thus, increasing the nonradioactive contribution to the aerosol mass suspended in the reactor containment is expected to increase the rate of decontamination by natural processes.

There is not now a highly reliable basis for estimating how much nonradioactive aerosol mass will be released to the containment atmosphere. The final version of NUREG-1465 does not provide quantitative guidance though an earlier draft suggested about three hundred kilograms

of nonradioactive mass might be released to containment during the in-vessel release phase of an accident. It is usually thought that temperatures are so low in the core region during the gap release phase of an accident, especially in a depressurized accident such as that considered here for the AP600, that not much nonradioactive material is vaporized from the reactor core. The nonradioactive source term becomes more important during the in-vessel release phase of an accident.

Because both the vaporization of radionuclides from fuel and the vaporization of nonradioactive materials are strongly influenced by temperature, it appears reasonable to assume as a first approximation that the nonradioactive aerosol mass will be proportional to the mass of radionuclides. The proportionality constant is, of course, quite uncertain.

Here, for the Monte Carlo uncertainty assessment, the proportionality constant between nonradioactive and radioactive aerosol mass during the gap release phase (0 to 1800 seconds) was taken to be log-uniformly distributed between 0.01 and 1.0. These relatively low values of the proportionality constant were selected to reflect the fact that temperatures in the core are low during the gap release phase of the accident so that vaporization of materials not intimately associated with reactor fuel ought to be low.

The proportionality constant between nonradioactive and radionuclide-bearing aerosol masses during in-vessel release is taken to be uniformly distributed between 0.5 and 2.0. The midpoint of this range approximates results obtained in accident analyses for NUREG-1150 [15] and the QUEST study [16]. The upper limit was chosen to acknowledge that past studies of aerosol production omitted some possible sources of nonradioactive aerosol mass. The lower bound on this range was chosen to reflect the fact that releases of nonradioactive aerosol are likely to be most extensive during the later stages of core degradation when it is more likely that aerosol formed in the reactor coolant system will not successfully negotiate a pathway to the reactor containment.

Analyses of aerosol behavior done with the NAUAHYGROS code assumed that the ratio of nonradioactive aerosol mass to radioactive aerosol mass was zero during the gap release phase of the accident and about 3.642 during the in-vessel release phase.

3. Thermal Conductivity of Aerosol Particles

The thermal conductivity of aerosol particles enters into the expression for the deposition velocity of aerosol particles by thermophoresis. This deposition velocity decreases with increasing thermal conductivity of the aerosol particle.

A general aerosol particle will be a porous conglomerate of primary particles which themselves may be composed of several chemical species. The thermal conductivities of such complicated materials have, of course, not been measured. Estimating the thermal conductivity of aerosol particles is complicated by the contact resistance between primary particles and the fact that liquid water fills the pore structure of the conglomerate.

For the Monte Carlo analysis an effective particle thermal conductivity, k(effective), is defined by:

$$k(\text{effective}) = \frac{\delta\varepsilon}{2k_3 d(pr) + \frac{1}{k_p}} + k_f (1 - \varepsilon)$$

where

ε = packing fraction (see subsection 5).
k_p = thermal conductivity of the primary particles
k_3 = $\varepsilon(k)k_p$ = contact zone thermal conductivity
δ = 0.1 d(pr)
d(pr) = diameter of the primary particles
k_f = thermal conductivity of water

Both the thermal conductivity of the primary particles and the thermal resistance of the contact zone between primary particles were taken to be uncertain.

The thermal conductivity of primary particles released during the gap release phase was assumed to fall within a range defined by the thermal conductivity of CsI (0.023 cal/cm-s-K) and the thermal conductivity of molten NaOH (0.0022 cal/cm s-K). During the in-vessel release phase metallic materials (Ag, Cd, In, Te and Fe) as well as oxidic materials (UO_2, U_3O_8, Fe_2O_3, etc.) may be released to the containment as aerosols. Consequently, the plausible range of values for the thermal conductivity of primary particles was expanded to 0.1 to $3x10^{-4}$ cal/cm-s-K.

The thermal conductivity of the contact region between particles is quite uncertain. It was assumed for the Monte Carlo calculations that this thermal conductivity would be proportional to the thermal conductivity of the primary particles. The proportionality constant is uncertain. A range of possible values was taken to be 0.5 (essentially no contact resistance) to 10^{-3} (only point contact between particles).

4. Particle Material Density

The material density of aerosol released to the containment is difficult to predict since the chemical forms of the radionuclides are not known and the nonradioactive aerosol mass is not identified. The material density during the gap release was taken to be uniformly distributed over the range 2.8 to 4.51 g/cm^3. This range spans measured densities of saturated CsOH solutions and solid CsI. The aerosol material density during the in-vessel release phase was taken to be log-uniformly distributed over the range 3.25 to 10.96 g/cm^3. This range allows for the possibility that uranium oxides may be major contributors to the aerosol. Note that the actual aerosol particle density is calculated recognizing the particles are porous (see subsection 5).

5. Shape Factors

Shape factors partially correct the aerosol physics equations for effects that arise because real aerosol particles are not perfectly dense spheres. Two shape factors arise in the analysis of aerosol behavior in reactor containments, the dynamic shape factor, χ, and the collision shape factor, γ. Because of the high humidity of the containment atmosphere, water in the pore structure of an aerosol particle composed of coagulated primary particles draws the agglomerate into a nearly spherical envelop so that the two shape factors are equal. Still, these shape factors do not have unit values. The shape factors are taken here to be:

$$\chi = \gamma = 1 / \alpha^{1/3}$$

where α is related to the packing density by:

$$\alpha = \frac{\varepsilon \rho_\rho + (1 - \varepsilon)\rho_f}{\rho_\rho}$$

where

ε = packing efficiency of primary particles,

ρ_ρ = primary particle material density, and

ρ_f = density of material that fills voids in the agglomeration of primary particles.

Here, it is assumed that because of curvature effects the voids within a particle are filled with liquid water. The packing efficiency of primary particles is estimated from a fractal model:

$$\varepsilon = \left(\frac{d_{pr}}{d_p} \right)^{3-d_f}$$

where

d_f = fractal dimension,

d_{pr} = diameter of primary aerosol particles, and

d_p = diameter of the primary particle agglomerate.

Thus, shape factors differ in general from unity and are dependent on particle size. The primary aerosol particles that agglomerate to make aerosol particles are not well understood. For the Monte Carlo uncertainty analysis, the primary particles were taken to have diameters log-uniformly distributed over the interval 0.02 to 0.2 μm. The fractal dimension of aerosol particles was taken to be uncertain over the range 1.5 to 2.2.

In the NAUAHYGROS point estimates of aerosol behavior shape factors were taken to be independent of particle size and equal to one.

6. Accommodation Coefficients

Because aerosol removal from the atmosphere of the AP600 containment involves phoretic processes (diffusiophoresis and thermophoresis) in such important ways, the momentum and the thermal accommodation coefficients associated with gas-surface interactions could be of some importance. These coefficients have not been measured for the particular combinations of gases and aerosol surfaces that can be expected to exist in the AP600 containment atmosphere under accident conditions.

Momentum accommodation coefficients have been measured at temperatures near 300K using Milliken oil-drop experimental techniques. These measurements for spherical, liquid (oil) droplets yield valves near 0.92. Measurements with solid particles have been reported as low as 0.7 at room temperature [4].

More data are available for thermal accommodation coefficients which can be measured in low-pressure heat transfer experiments. Some data for the thermal accommodation coefficients of various gasses on glass surfaces are shown in Figure 6 [4].

Theoretical analyses suggest that accommodation coefficients should be:

- temperature-dependent,
- lower for polyatomic gases such as steam than for monatomic gases such as helium,
- increase with the molecular weight of the gas, and
- momentum accommodation is more complete than thermal accommodation.

The accommodation coefficients are bounded by the values of 0 to 1 and momentum accommodation may be bounded by 0.5 and 1.0.

Useful, simple models for the accommodation coefficients that do not require assumptions or unavailable data about the nature of the particle surface seem not to exist. Consequently, for the Monte Carlo uncertainty analysis *ad hoc* expressions for the momentum and thermal accommodation coefficients that satisfy the suggestions obtained from theoretical analyses are used:

$$\alpha_m = 1.0 - A \exp(-300 / T(K))$$

$$\alpha_t = \frac{4(MW / 44)}{(1 + MW / 44)^2} \alpha_m \left(1 - A^1 \exp(-300 / T(K))\right)$$

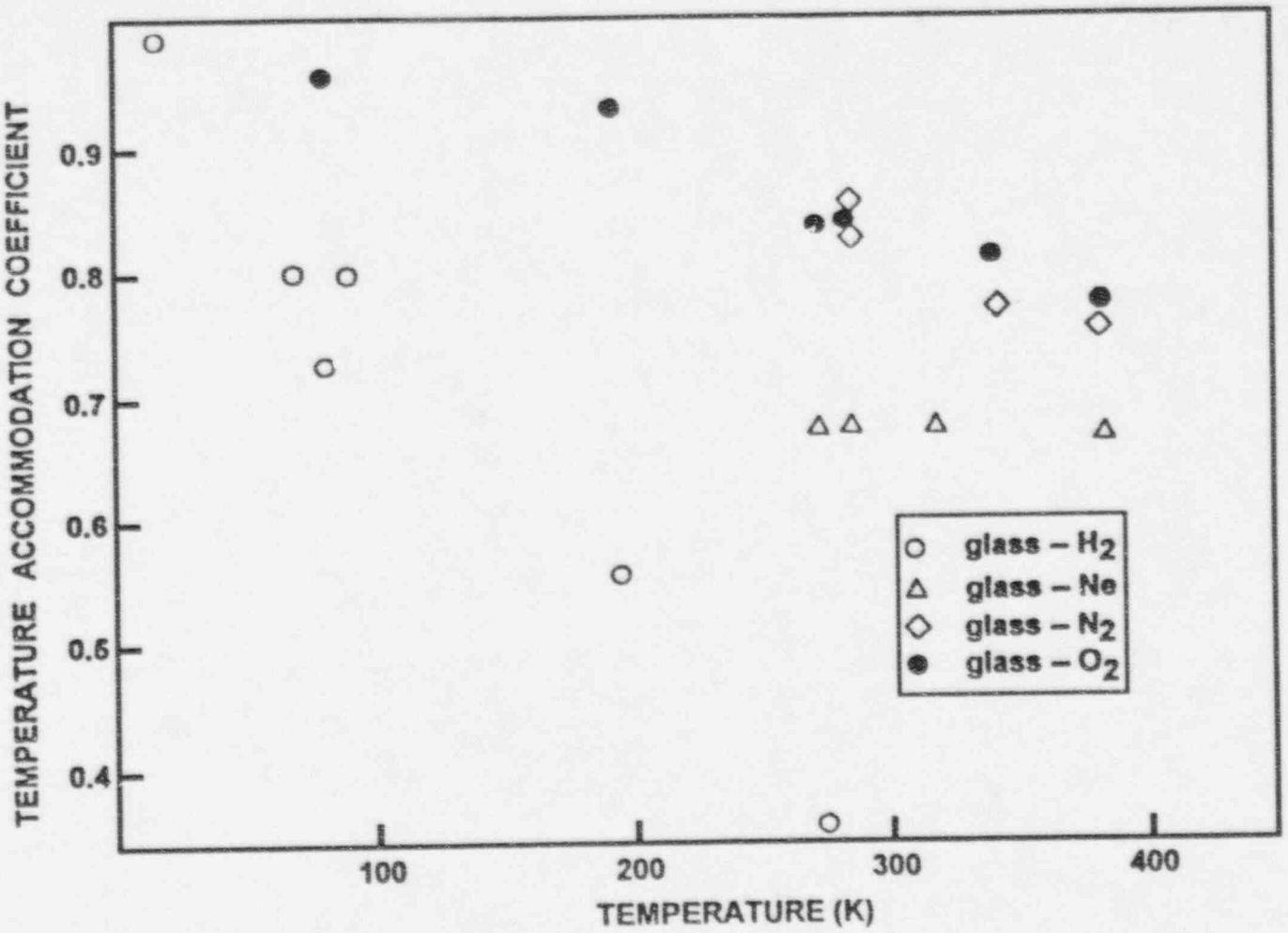

Figure 6. Thermal Accommodation Coefficients for Various Gases Interacting with Glass Surfaces as Functions of Temperature.

where

MW = average molecular weight of the gas,

A = uncertain parameter with values uniformly distributed over the interval from 0 to 0.6, and

A^1 = uncertain parameter with values uniformly distributed over the interval from 0 to 0.6.

This formulation makes the accommodation coefficients temperature-dependent and assures $\alpha_t < \alpha_m$.

The accommodation coefficients enter into the expressions for thermophoretic and diffusiophoretic deposition velocities. For instance, Talbot's model [4] of the thermophoretic deposition velocity is:

$$V_T = \frac{\frac{-2\ \mu_g C C_s}{\rho_g \chi}\left[\frac{k_g}{k_p} + C_t Kn\right] \nabla \ln T}{\left(1 + 3C_m Kn\right)\left[1 + \frac{2k_g}{k_p} + 2C_t Kn\right]}$$

where

μ_g = gas viscosity
ρ_g = gas density
k_g = gas thermal conductivity
k_p = effective particle thermal conductivity
Kn = Knudsen number
C = slip correction factor

The "jump" coefficients* C_s, C_t, and C_m in this expression are related to the thermal and momentum accommodation coefficients. The relationships between the accommodation coefficients and the parameters in the expression for the thermophoretic velocity is often derived based on a hard-sphere potential particle surface and the gas. For the Monte Carlo analysis, a more realistic Lennard-Jones potential was between the assumed. Then,

$$C_s = 0.75(1 - \alpha_m) + 3\alpha_m \xi(s)$$

*Note that in Reference 12 describing the results of calculations with the NAUAHYGROS code C_t is referred to as the thermal accommodation coefficient and C_m is called the momentum accommodation coefficient. This is not standard nomenclature and these parameters are certainly not the accommodation coefficients discussed here.

$$C_t = \frac{15}{8} \frac{(2 - \alpha_t)}{\alpha_t} \left[\left(1 - \alpha_t\right) \frac{5}{8} \sqrt{\pi} + \alpha_t \xi(m) \right]$$

$$C_m = \frac{(2 - \alpha_m)}{\alpha_m} \left[\left(1 - \alpha_m\right) \frac{\sqrt{\pi}}{2} + \alpha_m \xi(m) \right]$$

where

$\xi(s)$ = uncertain parameter with values uniformly distributed over the range 0.35 to 0.383

$\xi(t)$ = uncertain parameter uniformly distributed over the range 1.263 to 1.296, and

$\xi(m)$ = uncertain parameter uniformly distributed over the range 0.996 to 1.02.

Accommodation coefficients also enter into the expression used here for the slip correction factor:

$$C = \frac{15 + 12C_1Kn + g\left(C_1^2 + 1\right)Kn^2 + 18C_2\left(C^2 + 2\right)Kn^3}{15 - 3C_1Kn + C_2\left(8 + \pi\alpha_t\right)\left(C_1^2 + 2\right)Kn^2}$$

where

$$C_1 = \frac{\left(2 - \alpha_m\right)}{\alpha_m}, \text{ and}$$

$$C_2 = \frac{1}{\left(2 - \alpha_m\right)}$$

use of this expression for the slip correction factor provides a more realistic temperature dependence than do usual expressions of the form:

$$C = 1 + Kn[a + b \exp(-c / Kn)]$$

Finally, accommodation coefficients enter into the expression for the diffusiophoresis scattering kernal described in subsection 7.

7. Diffusiophoretic Scattering Kernal

The deposition velocity for aerosol particles due to diffusiophoresis is:

$$V_D = \frac{-C}{\chi}\left\{\frac{\chi}{C} + \sigma_{12}(1 - P(H_2O)/P_T)\right\}\frac{Đ(H_2O)}{P_T - P(H_2O)}\nabla P(H_2O)$$

where

$P(H_2O)$ = $P_T\, x(H_2O)$

$x(H_2O)$ = mole fraction steam in the atmosphere,

$Đ(H_2O)$ = diffusion coefficient of steam in air = $\frac{0.3106}{P_T}(T/373)^{1.82}$ cm^2/s,

P_T = total pressure

σ_{12} = diffusiophoretic scattering kernal,

C = slip correction factor, and

χ = dynamic shape factor

The diffusiophoretic scattering kernal is a source of uncertainty. Based on classic kinetic analysis treating gas molecules as hard spheres:

$$\sigma_{12}\,(\text{classic}) = \frac{m(H_2O) - m(air)}{m(air) + m(H_2O) + \left[m(H_2O)\, m(air)\right]^{1/2}}$$

where m(i) is the mass of a molecule of species i. Unfortunately, this description does not yield results that always fit well experimental data. A variety of alternative expressions have been developed. One of the most complete derivations [4] yields:

$$\sigma_{12}\,(KC) = \frac{m(H_2O)^{1/2} - m(air)^{1/2}\, Q(air)/Q(H_2O)}{m(air)^{1/2}\,\frac{Q(air)}{Q(H_2O)} + x(H_2O)\left[m(H_2O)^{1/2} - m(air)^{1/2}\,\frac{Q(air)}{Q(H_2O)}\right]}$$

where

$$Q(i) = 1 + \pi/8 - 0.5(1 - \alpha_m(i)) + \pi(1 - \alpha_t(i))/16$$

$\alpha_t(i)$ = thermal accommodation coefficient for species (i), and

$\alpha_m(i)$ = momentum accommodation coefficient for species (i).

Even this expression has not achieved widespread acceptance.

To account for the uncertainty in the diffusiophoretic scattering kernal, a parameter $\delta(\sigma_{12})$ was defined to have values uniformly distributed over the interval 0 to 1, and

$$\sigma_{12} = \begin{cases} \sigma_{12}(\text{classic}) & \text{for } \delta(\sigma_{12}) < 0.5 \\ \sigma_{12}(\text{KC}) & \text{for } \delta(\sigma_{12}) \geq 0.5 \end{cases}$$

8. Natural Convection Length Scale

A length scale, L, is required for the modeling of turbulent deposition of aerosol particles. This scale should be related to the geometry of the containment. Here, it was assumed that the length scale was proportional to the specified equivalent height of the containment. The proportionality constant was taken to be log-uniformly distributed over the interval from 0.1 to 1.0.

9. Turbulent Energy Dissipation Rate

The rate of turbulent energy dissipation enters into the calculation of particle coagulation by turbulent inertial processes and by turbulent diffusion. The turbulent energy dissipation rate in reactor containment atmospheres is, however, quite uncertain. Here this energy dissipation rate, ε, was taken to be:

$$\varepsilon = \varepsilon(t) A_v H / V$$

where

A_v = vertical surface area of containment,

H = effective height of containment,

V = volume of containment, and

$\varepsilon(t)$ is an uncertain parameter log-uniformly distributed over the interval from 2 to 20 cm^2/s^3.

10. Friction Velocity

A friction velocity is used in the calculation of turbulent deposition of aerosol particles. This friction velocity is given by:

$$u^* = \xi\sqrt{f/2}$$

where

ξ = uncertain parameter uniformly distributed over the range 0.1467 to 0.537,

$f = 0.045\ (\mu_g/\rho_g \lceil \delta)^{1/4}$

and $\lceil$ and δ are dimensionless quantities calculated as described in Section I-8.

III. RESULTS

A. EXAMPLE CALCULATION

Results of a single, typical calculation from the Monte Carlo uncertainty analysis of aerosol behavior in the AP600 reactor containment during the hypothesized 3BE accident are shown in Figures 7 and 8. These results were obtained using one particular set of values for the uncertain parameters discussed in the previous chapter. Some of the quantitative features of the predicted aerosol behavior are quite dependent on the selected values of these uncertain parameters. The results of this example calculations are, then, of only qualitative significance.

The overall decontamination coefficient is shown as a function of time in Figure 7. The variations of the overall decontamination coefficient with time parallel closely the variations with time of the rate of steam condensation from the containment atmosphere (see Figure 4). This suggests that aerosol deposition by diffusiophoresis is a dominant aerosol removal process.

Deposition velocities for aerosol particles by diffusiophoresis, thermophoresis, gravitational settling and turbulent inertial processes are compared in Figure 8. Indeed, these results show that throughout the accident, diffusiophoresis is the dominant aerosol removal mechanism. It is generally true that gravitational settling grows in importance as aerosol mass continues to be added to the containment atmosphere and particles grow. Eventually, gravitational settling becomes comparable to diffusiophoresis as a decontamination mechanism.

Particle growth is not rapid at the low total aerosol concentrations involved in this design-basis accident (see Figure 7). Consequently, gravitational settling velocities increase even after release of aerosols to the containment atmosphere stops at 6480 seconds. Gravitational settling most efficiently removes larger aerosol particles. As decontamination progresses, aerosol concentrations fall and large particles removed from the containment atmosphere are

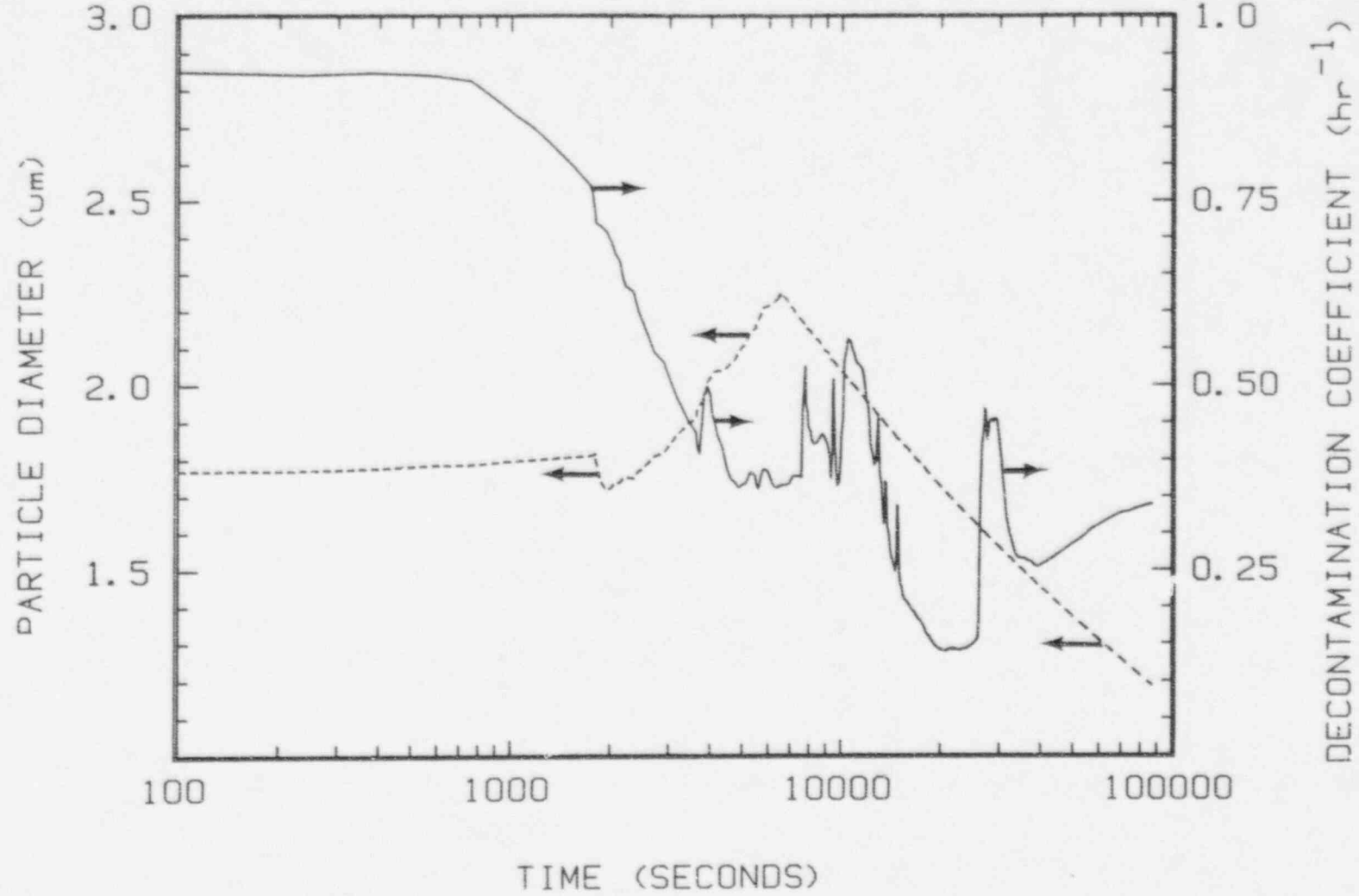

Figure 7. Overall Decontamination Coefficient (solid line) and Median Aerosol Particle Size (dashed line) as Functions of time for the Example Calculation.

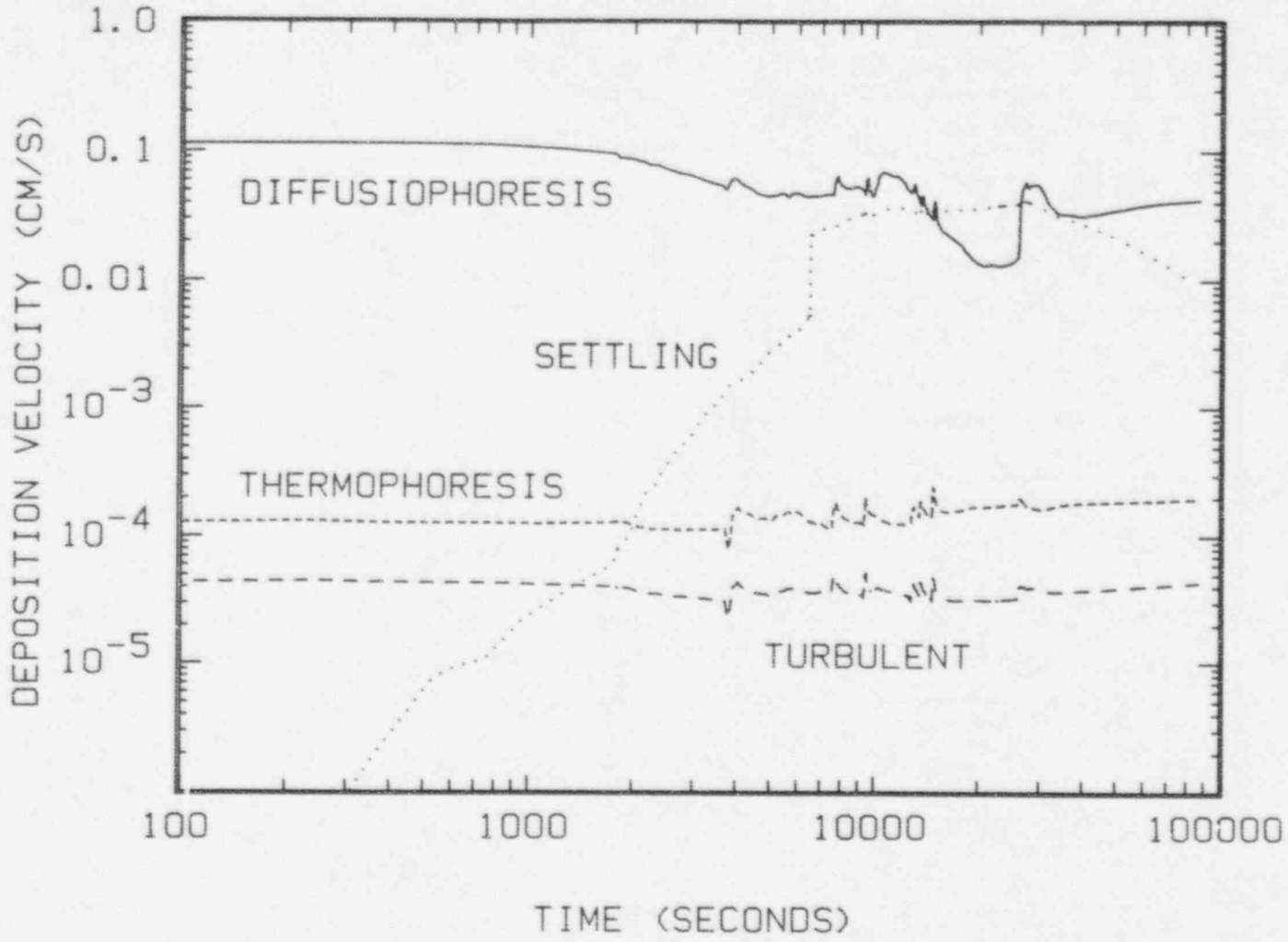

Figure 8. Deposition Velocities Due to Various Mechanisms as Functions of Time for the Example Calculation.

not rapidly replaced by aerosol growth. After some time, the rate of aerosol removal by gravitational settling reaches a maximum and then begins to decrease.

Thermophoretic deposition of particles and turbulent deposition are smaller contributors to the total rate of aerosol removal throughout the accident. If the convoluted surfaces within the reactor containment are neglected as they were in the specification of this problem, these processes do not make significant contributions to the aerosol removal by natural processes.

Diffusiophoresis was found for these calculations of aerosol behavior in the AP600 containment to be an important aerosol removal mechanism at the start of the accident and to remain important throughout the calculation. This contrasts with findings for analyses of aerosol behavior in the containments of existing light water reactors in which diffusiophoresis waned in importance as the accident progressed [4]. External cooling of the AP600 containment keeps steam condensation and, consequently, aerosol deposition by diffusiophoresis high throughout the accident. The rates of steam condensation and diffusiophoretic deposition of aerosols are calculated to fall over the course of an accident in an existing light water reactor as the containment surfaces rise in temperature.

B. MONTE CARLO UNCERTAINTY ANALYSIS

Calculations similar to that described in the previous subsection were repeated using different values of the uncertain parameters and the results accumulated to develop uncertainty distributions for the predicted aerosol behavior. Calculations, or sampling of the uncertainty distributions, was continued until there was a 99 percent confidence that 95 percent of the range of predicted aerosol behavior had been sampled.

Uncertainty distributions were developed for the decontamination factors for both gap release and in-vessel release materials at five selected times--1800, 6480, 13600, 49680 and 86450 seconds. The accumulated values of these decontamination factors were analyzed using nonparametric order statistics to develop uncertainty distributions at selected levels of confidence. More details on the construction of these uncertainty distributions are presented in Appendix A of Reference 5. The uncertainty distributions consist of ranges of values that correspond to percentiles of the distribution. Percentiles so characterized are at 5 percent intervals from 5 percent to 95 percent. The widths of the ranges of values depend on the selected confidence level. Here, distributions were developed for confidence levels of 50 and 90 percent. That is, there is a 50 and a 90 percent confidence, respectively, that the true value of the decontamination factor corresponding to the specified percentile of the distribution falls within the indicated ranges and, consequently, a 50 and a 10 percent probability, respectively, that the true value is above or below the indicated range.

An example uncertainty distribution is shown in tabulated form in Table 3. Tabulations of other distributions generated in this work are collected in Appendix B. Distributions for the decontamination factors for gap release material at various times are shown graphically in Figure 9.

Table 3. Uncertainty Distribution of the Decontamination Factor for Gap Release Material at 86450 Seconds.

	Values of the Decontamination Factor Characteristic of the Indicated Percentile at a Confidence Level, C, of	
Percentile	C= 90%	C=50%
5	509.4 to 728.8	565.8 to 640.4
10	633.6 to 820.4	729.8 to 774.2
15	757.5 to 921.4	804.8 to 837.6
20	821.4 to 980.2	840.6 to 933.1
25	900.1 to 1029	933.1 to 992.3
30	951.0 to 1087	993.7 to 1062
35	1010 to 1165	1061 to 1117
40	1069 to 1418	1110 to 1278
45	1156 to 1554	1259 to 1465
50	1283 to 1622	1439 to 1568
55	1476 to 1746	1567 to 1651
60	1584 to 1897	1637 to 1748
65	1663 to 2145	1747 to 1964
70	1750 to 2319	1958 to 2198
75	1981 to 2560	2200 to 2394
80	2226 to 2673	2405 to 2604
85	2517 to 3118	2605 to 3002
90	2730 to 3816	3052 to 3488
95	3488 to 4515	3816 to 4011

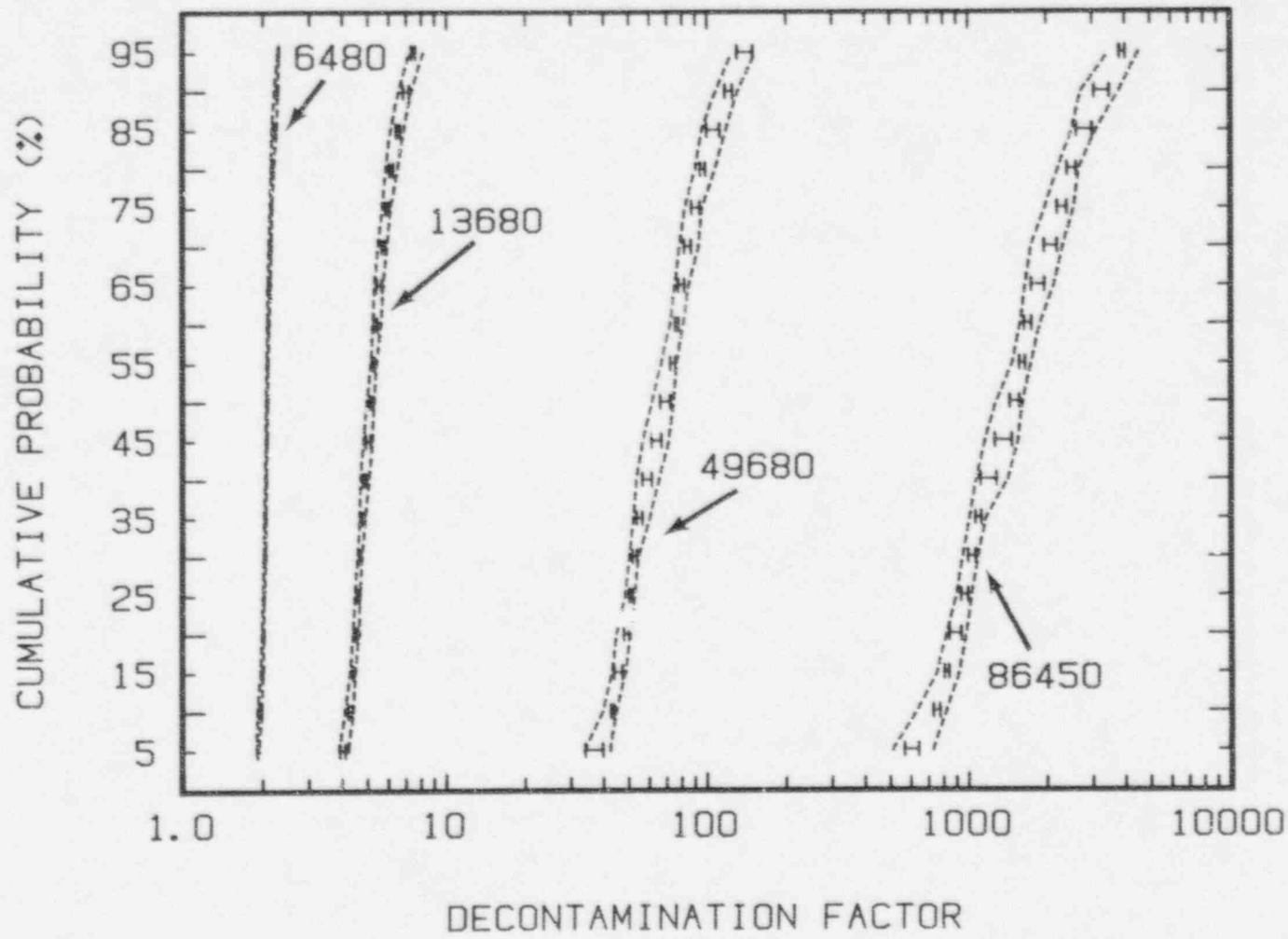

Figure 9. Uncertainty Distributions for the Gap Release Decontamination Factor at Selected Times.

The uncertainty distributions can be summarily described in terms of values for selected percentiles. Here the median or 50 percentile value is taken to be the "best estimate" of the decontamination factor. "Reasonable upper bound" and "reasonable lower bound" values are taken to be the 90 and 10 percentile values, respectively. These features of the various uncertainty distributions for the decontamination factors are summarized in Table 4. Also shown in the table are mean values which are of interest to some.

For some purposes, the effective decontamination coefficient is of more interest than the decontamination factor. Effective decontamination coefficients, $\lambda_e(t)$, are parameters that arise in the formal differential equation:

$$\frac{d\ DF(t)}{dt} = \lambda_e(t)\ DF(t)$$

where DF(f) is the decontamination factor.

The effective decontamination coefficients are distinct from instantaneous decontamination coefficients, $\lambda(t)$, that are parameters in the formal differential equation:

$$\frac{d\ M(t)}{dt} = -\ \lambda(t) M(t) + \dot{S}(t)$$

where

$M(t)$ = suspended aerosol mass, and
$\dot{S}(t)$ = aerosol source to the containment.

The effective decontamination coefficient subsumes the effects of any aerosol source term. Consequently, when a source is active the effective decontamination coefficient is less than the instantaneous decontamination coefficient. When there is no source term, the effective decontamination coefficient and the instantaneous decontamination coefficient are the same.

Here, effective decontamination coefficients for selected time intervals from t(i) to t(f) were calculated from:

$$\ln \frac{DF(t(f))}{DF(t(i))} = \lambda_e\,[t(f) - t(i)]$$

where

$DF(t)$ = decontamination factor at time t, and
λ_e = effective decontamination coefficient.

These effective decontamination coefficients average over the substantial, transient variations in the decontamination coefficients shown in Figure 7 for an example calculation. Notice that this formulation for the effective decontamination coefficient subsumes that source rate as a process that mitigates decontamination. Therefore, during periods of aerosol release, it is

Table 4. Summary of Uncertainty Distributions of the Decontamination Factors at Selected Times

	Range of Values of DF(t) Corresponding to Various Percentiles, P, of the Uncertainty Distributions			
Time (s)	Mean	Best Estimate* (P=50%)	Upper Bound** (P=90%)	Lower Bound** (P=10%)
Gap Release				
1800	1.2055	1.204 - 1.205	1.222 - 1.229	1.183 - 1.192
6480	2.0921	1.075 - 1.087	2.219 - 2.291	1.910 - 1.984
13680	5.3641	5.100 - 5.241	6.580 - 7.328	4.108 - 4.412
49680	74.27	65.99 - 72.22	108.2 - 131.1	39.74 - 44.8
86450	1740	1439 - 1568	2730 - 3816	633.6 - 820.4
In-Vessel Release				
6480	1.2615	1.260 - 1.261	1.286 - 1.302	1.222 - 1.240
13680	3.227	3.096 - 3.145	4.217 - 4.295	2.583 - 2.719
49680	44.96	38.85 - 43.16	65.17 - 77.35	25.30 - 27.63
86450	1034	878.3 - 946.6	1600 - 21.67	399.5 - 507.5

*50% confidence level.
**90% confidence level.

possible to get decontamination coefficients that are not positive, though this did not occur in the calculations reported here. The formulation for the effective decontamination coefficients does mean that during the period of in-vessel release there are distinct values of the effective decontamination coefficient for gap release material and the effective decontamination coefficient for in-vessel release material. After 6480 seconds, the effective decontamination coefficients for these materials are the same.

Results of the Monte Carlo analyses were recalculated in terms of the effective decontamination coefficients for the time intervals 0-1800, 1800-6480, 6480-13680, 13680-49680, 49680-86450 seconds. The uncertainty distributions for these effective decontamination coefficients are summarily described in Table 5. The detailed uncertainty distributions are listed in Appendix B. Uncertainty distributions for the effective decontamination coefficients for gap release material during selected time intervals are shown in Figure 10.

The distributions found for the decontamination factors and the effective decontamination coefficients for the 3BE accident in the AP600 reactor are narrower than distribution found in analysis of generalized accidents at existing light water reactors [4]. Typically, conservative, lower bound values of the effective decontamination coefficient are only 10 to 15 percent less than the median or best estimate values. This, of course, is because the accident boundary conditions have been fixed in the calculations for the AP600 reactor accident. Boundary conditions have such important effects on aerosol behavior that uncertainties in boundary conditions during hypothesized accidents at existing light water reactors contribute significantly to uncertainties in predictions of aerosol behavior.

The effective decontamination coefficients found in the uncertainty analysis for the 3BE accident are compared in Table 6 to those found in the preliminary analysis. The effective decontamination coefficients found for the 3BE accident are substantially larger than values found in preliminary analyses. This is because continued cooling of the containment shell of the AP600 reactor maintains high rates of steam condensation. Consequently, there is a high rate of diffusiophoretic aerosol deposition from the containment atmosphere. In analyses of aerosol behavior in existing light water reactors, the containment boundary is heated so that diffusiophoresis makes a decreasing contribution to aerosol removal as an accident progress.

C. COMPARISON TO NAUAHYGROS RESULTS

Predictions of aerosol behavior in the 3BE accident obtained with the NAUAHYGROS computer model are available as tabulated values of the instantaneous decontamination coefficient. These values are plotted in Figure 11 against time. The decontamination coefficients shown in this figure have some qualitative similarity to the values shown in Figure 7 for an example calculation with the model used for the Monte Carlo uncertainty analysis. That is, there is a fairly smooth decrease in the decontamination coefficient over the interval 0 to 1800 seconds. After about 3500 seconds, there are sharp variations in the decontamination coefficient that parallel variations in the boundary conditions. The most striking difference in the variations of the decontamination coefficient with time calculated with the NAUAHYGROS code and values of the decontamination coefficients calculated for

Table 5. Summary of Uncertainty Distributions of the Effective Decontamination Coefficients

Time interval (s)	Range of Values of $\lambda_e(hr^{-1})$ Corresponding to Various Percentiles, P, of the Uncertainty Distributions			
	Mean	Best Estimate* (P = 50%)	Upper Bound** (P = 90%)	Lower Bound** (P = 10%)
0-1800	0.374	0.371 to 0.373	0.402 to 0.413	0.336 to 0.351
1800-6480 (gap release)	0.423	0.419 to 0.422	0.458 to 0.479	0.368 to 0.392
1800 to 6480 (In-vessel release)	0.178	0.178 to 0.178	0.193 to 0.203	0.154 to 0.166
6480 to 13680	0.463	0.443 to 0.455	0.566 to 0.604	0.371 to 0.397
13680 to 49680	0.257	0.257 to 0.262	0.279 to 0.290	0.225 to 0.232
49680 to 86450	0.301	0.297 to 0.299	0.327 to 0.340	0.267 to 0.279

*at 50% confidence.
**at 90% confidence.

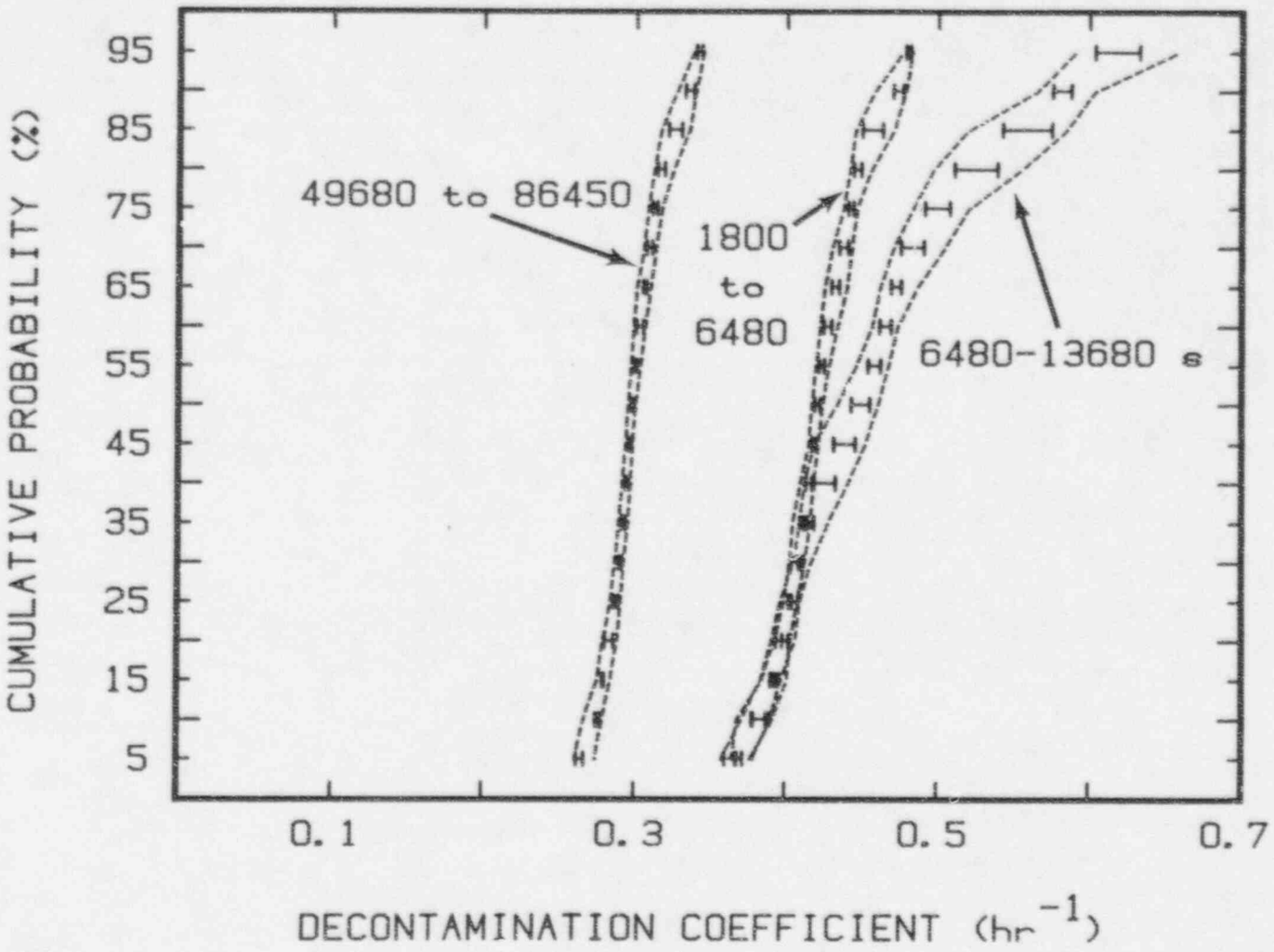

Figure 10. Uncertainty Distributions for the Effective Decontamination Coefficients for Gap Release Material at Selected Times.

Table 6. Comparison of Effective Decontamination Coefficients Found for the 3BE Accident to those Found in the Preliminary Analysis

	$\lambda_e(hr^{-1})$ for 3BE Accident		$\lambda_e(hr^{-1})$ from Preliminary Analysis	
Time Interval (s)	Best Estimate	10 to 90 Percentile Range	Best Estimate	10 to 90 Percentile Range
0-1800	0.372 ± 0.001	0.336 to 0.413	0.0335	0.0245 to 0.0434
1800-6480 (gap release)	0.420 ± 0.001	0.368 to 0.479	0.0383	0.0270 to 0.0517
1800 to 6480 (In-vessel release)	0.178 ± 0.001	0.154 to 0.203	0.0733	0.054 to 0.102
6480 to 13680	0.449 ± 0.006	0.371 to 0.604	0.170	0.0765 to 0.418
13680 to 49680	0.260 ± 0.003	0.225 to 0.290	0.151	0.101 to 0.189
49680 to 86450	0.298 ± 0.001	0.267 to 0.340	0.0912	0.085 to 0.101

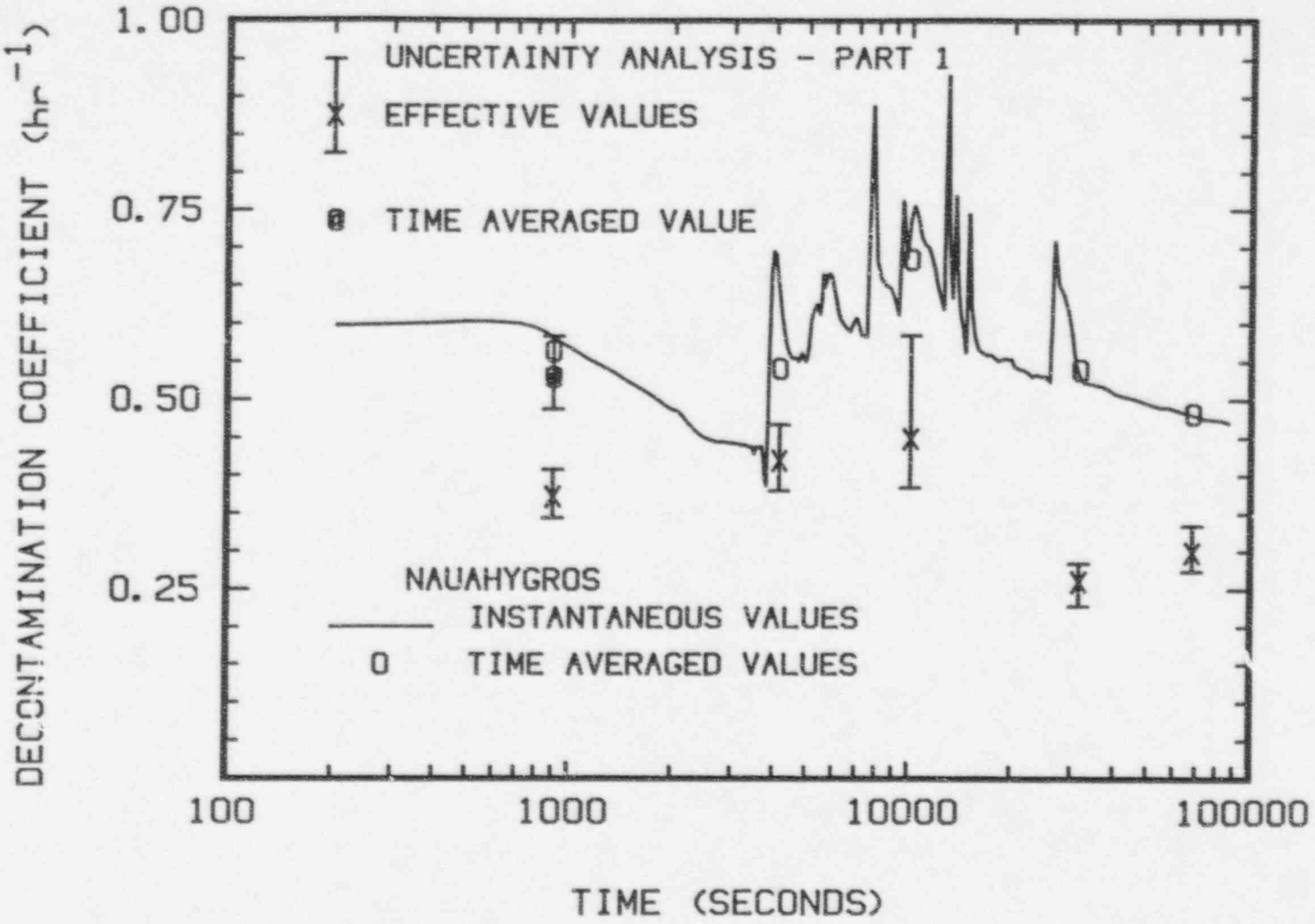

Figure 11. Instantaneous Values of the Decontamination Coefficient Calculated with the NAUAHYGROS Computer Code. Time-average values of the decontamination coefficients are plotted as open symbols. Effective decontamination coefficients calculated in the uncertainty analysis are shown as filled symbols.

the example calculation shown in Figure 7 is that values calculated with NAUAHYGROS for times greater than about 6000 seconds are noticeably higher. Also, at late times, the decontamination coefficients calculated with NAUAHYGROS vary less with variations in the boundary conditions than do values found in the uncertainty analysis calculations.

The tabulated values of the decontamination coefficients calculated with the NAUAHYGROS computer model reflect the significant variations with time in the boundary conditions including the transient spikes in these boundary conditions. To compare results obtained with the NAUAHYGROS computer code to the uncertainty distributions obtained here for the effective decontamination coefficients, the instantaneous values of the decontamination coefficients were time-averaged over the intervals 0-1800, 1800-6480, 6480-13680, 13680-49680 and 49680-86450 seconds. These average values are plotted at the midpoint of their respective time intervals as open symbols in Figure 11. The values are compared to the medians, upper bounds and lower bounds of the uncertainty distributions for the effective decontamination coefficients in Table 7. Note that the comparison is not quite appropriate for the 0-1800 second interval. Values for the effective decontamination coefficient during this time interval include the effect of the gap release which is not included in the averaged values of the instantaneous decontamination coefficient. Other comparisons shown in the table including that for the 1800 to 6480 second time interval are not affected by the release.

A second uncertainty analysis was done to compute the uncertainty distribution for the time-averaged decontamination coefficient for the 0 to 1800 second period that could be directly compared to results of the NAUAHYGROS calculation. This second uncertainty analysis yielded a median time-averaged decontamination coefficient of 0.530 hr^{-1}. The 10 percentile and 90 percentile values were found to be 0.488 and 0.585 hr^{-1}, respectively. These values can be compared to 0.564 $\pm$ 0.007 hr^{-1} found for the 0 to 1800 second interval with the NAUAHYGROS computer code. This point value found with the NAUAHYGROS code falls at about the 80 percentile the uncertainty range found in the uncertainty analysis. It is evident then that the discrepancies between results obtained with the NAUAHYGROS computer code and results of the uncertainty analysis are not enormous at the beginning of the accident calculation, but these discrepancies increase as the accident calculation progresses.

Though the effective decontamination coefficients calculated in the Monte Carlo analysis of the 3BE accident are larger than what was calculated with general and uncertain boundary condition [4], they are not as large as values calculated with the NAUAHYGROS computer code [12]. In fact, values calculated with NAUAHYGROS for times after 1800 seconds exceed the 90 percentile of the uncertainty distributions calculated here.

The discrepancy between values calculated in the Monte Carlo uncertainty analysis and values calculated with the NAUAHYGROS code increases as the accident progresses until the last time interval considered here, 49680 to 86450 seconds. Decontamination coefficients calculated with the NAUAHYGROS code remain high in the later phases of the accident. The reasons for this are not yet known, but it is likely that gravitational settling makes a bigger predicted contribution to aerosol removal in the NAUAHYGROS calculations because a much larger nonradioactive source term of aerosols has been hypothesized for the NAUAHYGROS calculations than the range of nonradioactive source terms considered in the Monte Carlo uncertainty analysis. Calculations to confirm this speculation have been initiated.

Table 7. Comparison of Effective Decontamination Coefficients to Averaged Values Obtained with the NAUAHYGROS Code

Time Interval (s)	Time-Averaged Instantaneous Values From NAUAHYGROS* (hr^{-1})	Effective Decontamination Coefficient (hr^{-1})		
		Median† (50 percentile)	Upper Bound† (90 percentile)	Lower Bound† (10 percentile)
0-1800**	0.5645 ± 0.0074	0.372 ± 0.001	0.408 ± 0.006	0.344 ± 0.008
1800-6480	0.5410 ± 0.0091	0.420 ± 0.002	0.468 ± 0.010	0.380 ± 0.012
6480-13680	0.6849 ± 0.0152	0.449 ± 0.006	0.585 ± 0.019	0.384 ± 0.013
13680-49680	0.5392 ± 0.0082	0.260 ± 0.003	0.284 ± 0.006	0.228 ± 0.004
49680-86450	0.4816 ± 0.0032	0.298 ± 0.001	0.334 ± 0.006	0.273 ± 0.005

*Standard deviation cited here is the square root of the time-weighted variance about the mean.

**Effective decontamination coefficients for the 0-1800 s interval include the effect of gap release and are expected to be less than the time weighted average of instantaneous values.

†Value is the midpoint of the range and the listed uncertainties define the range which is a 50 percent confidence interval for the median and a 90 percent confidence interval for the upper and lower bounds.

IV. CONCLUSIONS

Boundary conditions appropriate for accidents in the AP600 reactor significantly increase the predicted effective decontamination coefficients by natural aerosol processes from values calculated in preliminary analyses. The increase is due to enhanced diffusiophoresis that is maintained throughout the accident by cooling the containment shell. Fixing the boundary conditions so that they do not vary in the Monte Carlo sampling to construct uncertainty distributions significantly narrows the distributions found for the effective decontamination coefficients.

Establishing the validity of the boundary conditions for the 3BE accident that produce the higher rates of aerosol removal is outside the domain of work considered here.

Though higher effective decontamination coefficients have been calculated using fixed boundary conditions for a particular, hypothetical accident, these decontamination coefficients are still smaller than decontamination coefficients calculated for the same accident with the NAUAHYGROS code. The decontamination coefficients calculated with the NAUAHYGROS code exceed the 90 percentiles of the uncertainty distributions for the effective decontamination coefficients calculated here. The cause of the remaining discrepancies has not been positively identified. The nature of the discrepancies suggests that NAUAHYGROS is predicting more aerosol removal by gravitational settling than is the model used for the Monte Carlo uncertainty analysis. A much larger source term of nonradioactive aerosol mass has been hypothesized in the NAUAHYGROS analysis of the 3BE accident than that used in the Monte Carlo calculations. This larger, nonradioactive source term may be responsible for predictions of larger decontamination coefficients by the NAUAHYGROS code. An additional set of calculations to confirm this speculation has been initiated.

V. REFERENCES

1. L. Soffer, et al., Accident Source Terms for Light-Water Nuclear Power Plants, NUREG-1465, U.S. Nuclear Regulatory Commission, Washington, D.C. 1995.

2. J. J. DiNunno, et al., Calculation of Distance Factors for Power and Test Reactor Sites, TID-14844, U.S. Atomic Energy Commission, Washington, D.C. 1962.

3. D. A. Powers and S. B. Burson, A Simplified Model of Aerosol Removal by Containment Sprays, NUREG/CR-5966, SAND92-2689, Sandia National Laboratories, Albuquerque, NM, June 1993.

4. D. A. Powers, K. E. Washington, S. B. Burson, and J. L. Sprung, A Simplified Model of Aerosol Removal by Natural Processes in Reactor Containments, NUREG/CR-6189, SAND94-0407, Sandia National Laboratories, Albuquerque, NM.

5. D. A. Powers and J. L. Sprung, A Simplified Model of Aerosol Scrubbing by a Water Pool Overlying Core Debris Interacting with Concrete, NUREG/CR-5901, SAND92-1422, Sandia National Laboratories, Albuquerque, NM, August 1992.

6. D. A. Powers, Source Term Attenuation by Water in The Mark I. Boiling Water Reactor Drywell, NUREG/CR-5878, SAND92-2688, Sandia National Laboratories, Albuquerque, NM, September 1993.

7. R. S. Denning, et al., Radionuclide Release Calculations for Selected Severe Accident Scenarios, PWR, Subatmospheric Containment Design, NUREG/CR-4624, BMI-2139, Vol. 3, Battelle's Columbus Division, Columbus, Ohio, July 1986.

8. R. S. Denning, et al., Radionuclide Release Calculations for Selected Severe Accident Scenarios, PWR Large Dry Containment Design. NUREG/CR-4624 BMI-2139, Vol. 5, Battelle's Columbus Division, Columbus. Ohio, July 1986.

9. R. S. Denning, et al., Radionuclide Release Calculations for Selected Severe Accident Scenarios, Supplemental Calculations, NUREG/CR-4624, BMI-2139, Vol. 6, Battelle's Columbus Division, Columbus, Ohio, August 1990.

10. M. T. Leonard, et al., Supplemental Radionuclide Release Calculations for Selected Severe Accident Scenarios, NUREG/CR-5062, BMI 2160, Battelle Columbus Division, Columbus, Ohio, February 1988.

11. J. A. Gieseke, et al., Radionuclide Release Under Specific LWR Accident Conditions Volume V, PWR-Large, Dry Containment Design (Surry Plant Recalculations) BMI-2104, Volume V, Battelle Columbus Laboratories, Columbus, Ohio, July 1984.

12. Letter from N. J. Liparulo to T. R. Quary, dated April 7, 1995, entitled, "Information Requested by RAI 40.23 Regarding Input Parameters for the Calculation of Aerosol Removal Coefficients, NTD-NRC-95-4430, DCP/NRC0302, Docket No. STN-52003.

13. R. Sher and J. Jokiniemi, NAUAHYGROS 1.0: A Code for Calculating the Behavior of Hygroscopic and Nonhygroscopic Aerosols in Nuclear Power Plant Containments Following a Severe Accident, EPRI TR-102775, Electric Power Research Institute, Palo Alto, CA, 1993.

14. M. L. Corradini, Nuclear Technology 64 (1984) 186.

15. Office of Nuclear Regulatory Research, Severe Accident Risks: An Assessment for Five U. S. Nuclear Power Plants, NUREG-1150, U.S. Nuclear Regulatory Commission, Washington, D.C., June 1989.

16. R. J. Lipinski, et al., Uncertainty in Radionuclide Release Under Specific LWR Accident Conditions, SAND84-0410, Volume 2, Sandia National Laboratories, Albuquerque, NM, February 1985.

APPENDIX A. TABULATIONS OF BOUNDARY CONDITIONS INPUT TO THE MECHANISTIC MODEL USED FOR THE MONTE CARLO UNCERTAINTY ANALYSIS

Tabulated values for the 3BE accident boundary conditions:

- containment pressure
- containment atmosphere temperature
- mole fraction steam in the containment atmosphere
- rate of steam condensation from the containment atmosphere
- rate of heat removal from the containment atmosphere

were provided by Westinghouse Electric Corporation. These boundary condition specifications were input to the mechanistic model of aerosol behavior and held invariant during the uncertainty analyses. The tabulated values are reproduced from the mechanistic code so that they may be checked for accuracy.

The tabulated values were used in the units as provided except atmosphere temperatures were converted from celsius to Kelvin by adding 273.15 and heat removal rates were converted from ergs/second to calories/second by dividing by 4.184×10^7.

Linear interpolation of the tabulated values was used to provide values for the fourth order Runge-Kutta routine with automatic step-size control used to solve the aerosol behavior equations. Plotted values in Figures 1 - 6 of the main text were also generated by the linear interpolation process.

Table A-1. Containment Pressure

	TIME (SECONDS)	PRESSURE (atm)		TIME (SECONDS)	PRESSURE (atm)
1	0	2.293	41	5221	1.870
2	725	2.277	42	5631	1.899
3	930	2.255	43	5731	1.917
4	1034	2.241	44	5931	1.905
5	1140	2.226	45	6031	1.891
6	1243	2.212	46	7651	2.089
7	1346	2.196	47	7761	2.010
8	1449	2.180	48	7861	1.968
9	1551	2.162	49	7971	1.942
10	1655	2.145	50	8081	1.925
11	1758	2.126	51	8281	1.912
12	1861	2.107	52	8891	1.898
13	1965	2.087	53	8991	1.882
14	2066	2.070	54	9091	1.866
15	2167	2.050	55	9191	1.851
16	2267	2.032	56	9291	1.836
17	2368	2.015	57	9391	2.029
18	2468	1.999	58	9491	1.941
19	2568	1.984	59	9591	1.888
20	2670	1.968	60	9691	1.855
21	2772	1.956	61	9791	1.872
22	2874	1.940	62	9891	1.900
23	2976	1.925	63	9991	1.936
24	3076	1.912	64	10090	1.975
25	3178	1.897	65	10190	1.998
26	3279	1.884	66	11100	1.988
27	3379	1.871	67	11500	1.974
28	3480	1.858	68	11700	1.958
29	3581	1.847	69	11800	1.946
30	3682	1.835	70	11910	1.931
31	3882	1.974	71	12010	1.915
32	3983	1.996	72	12110	1.897
33	4085	1.952	73	12210	1.881
34	4188	1.912	74	12310	1.865
35	4289	1.886	75	12410	1.851
36	4391	1.867	76	12510	1.838
37	4491	1.852	77	12710	1.816
38	4701	1.835	78	12810	1.989
39	4911	1.825	79	12910	1.911
40	5111	1.851	80	13010	1.859

Table A-1. Containment Pressure (Continued)

	TIME (SECONDS)	PRESSURE (atm)		TIME (SECONDS)	PRESSURE (atm)
81	13110	1.827	121	18750	1.424
82	13210	1.799	122	19050	1.415
83	13310	1.777	123	19360	1.407
84	13420	1.762	124	19860	1.396
85	13520	1.903	125	20160	1.388
86	13620	1.831	126	20760	1.380
87	13720	1.787	127	21570	1.373
88	13820	1.752	128	22370	1.365
89	13920	1.728	129	23670	1.358
90	14020	1.710	130	24980	1.366
91	14120	1.697	131	25780	1.376
92	14220	1.678	132	25880	1.416
93	14320	1.667	133	25980	1.497
94	14430	1.657	134	26080	1.564
95	14530	1.648	135	26180	1.596
96	14630	1.639	136	26280	1.615
97	14730	1.920	137	26380	1.627
98	14830	1.796	138	26480	1.638
99	14930	1.724	139	26580	1.648
100	15030	1.678	140	26680	1.660
101	15130	1.645	141	26780	1.673
102	15230	1.622	142	26880	1.687
103	15330	1.604	143	26990	1.697
104	15430	1.588	144	27590	1.708
105	15530	1.576	145	27790	1.723
106	15630	1.565	146	27990	1.735
107	15730	1.555	147	28290	1.744
108	15840	1.547	148	28700	1.755
109	15940	1.539	149	29800	1.745
110	16140	1.530	150	30000	1.734
111	16240	1.521	151	30200	1.720
112	16440	1.511	152	30400	1.705
113	16640	1.500	153	30600	1.692
114	16840	1.489	154	30800	1.679
115	17140	1.479	155	31000	1.667
116	17440	1.470	156	31200	1.655
117	17650	1.461	157	31410	1.643
118	17850	1.453	158	31610	1.633
119	18050	1.444	159	31810	1.623
120	18450	1.432	160	32110	1.611

Table A-1. Containment Pressure (Concluded)

	TIME (SECONDS)	PRESSURE (atm)
161	32410	1.600
162	32710	1.590
163	33010	1.582
164	33410	1.574
165	33910	1.566
166	34920	1.558
167	36120	1.550
168	37820	1.542
169	42940	1.550
170	44940	1.558
171	47150	1.566
172	49250	1.574
173	51460	1.582
174	53770	1.590
175	55980	1.598
176	58990	1.606
177	62800	1.615
178	67610	1.624
179	72830	1.633
180	78860	1.642
181	86490	1.649

Table A-2. Containment Atmosphere Temperature

	TIME (SECONDS)	TEMPERATURE (K)		TIME (SECONDS)	TEMPERATURE (K)
81	12110	381.1	121	18450	381.3
82	12210	380.3	122	18650	382.5
83	12310	379.6	123	18750	381.8
84	12410	379.0	124	18950	382.8
85	12810	415.9	125	19050	282.0
86	12910	409.2	126	19260	382.8
87	13010	401.2	127	19360	381.9
88	13110	396.0	128	19860	380.9
89	13210	391.4	129	20160	379.8
90	13310	388.7	130	20360	379.1
91	13420	386.9	131	20760	378.5
92	13520	424.2	132	20860	379.1
93	13620	412.5	133	20960	378.2
94	13720	403.9	134	21070	378.9
95	13820	397.1	135	21170	378.0
96	13920	393.1	136	21270	378.7
97	14020	390.3	137	21370	377.8
98	14120	388.3	138	21470	378.5
99	14220	385.9	139	21570	377.6
100	14320	384.8	140	21670	378.2
101	14430	384.1	141	21770	377.3
102	14530	383.5	142	21870	378.0
103	14730	467.6	143	21970	377.2
104	14830	437.1	144	22570	376.4
105	14930	419.3	145	22670	377.0
106	15030	407.9	146	22770	376.3
107	15130	400.3	147	23170	377.2
108	15230	395.0	148	23270	376.3
109	15330	391.4	149	23370	377.0
110	15430	388.6	150	23470	376.2
111	15530	386.6	151	25180	375.2
112	15630	385.0	152	25280	375.9
113	15730	383.7	153	25380	375.3
114	15840	382.8	154	25480	376.2
115	15940	382.0	155	25580	375.5
116	16040	381.2	156	25780	376.4
117	16340	380.3	157	25880	379.8
118	16540	381.0	158	25980	384.4
119	16640	380.4	159	26080	386.7
120	18250	382.3	160	26280	385.4

Table A-2. Containment Atmosphere Temperature (Continued)

	TIME (SECONDS)	TEMPERATURE (K)		TIME (SECONDS)	TEMPERATURE (K)
1	0	380.8	41	7651	429.8
2	621	380.1	42	7761	423.2
3	1140	379.5	43	7861	413.2
4	1551	378.7	44	7971	406.5
5	1758	377.7	45	8081	401.6
6	1965	376.6	46	8181	398.7
7	2167	374.8	47	8281	396.5
8	2976	374.2	48	8381	394.7
9	3581	373.6	49	8481	393.4
10	3782	375.5	50	8581	392.5
11	3882	406.4	51	8691	391.4
12	3983	417.9	52	8791	390.5
13	4085	411.6	53	8891	389.1
14	4188	404.7	54	8991	387.4
15	4289	400.6	55	9091	386.0
16	4391	397.8	56	9191	384.7
17	4491	395.9	57	9291	383.4
18	4701	394.4	58	9391	419.5
19	5011	396.6	59	9491	416.7
20	5111	402.2	60	9591	408.1
21	5221	407.6	61	9691	402.4
22	5331	408.3	62	9791	401.7
23	5631	415.5	63	9891	400.8
24	5731	420.7	64	10090	399.4
25	5931	416.7	65	10190	397.7
26	6031	411.6	66	10300	395.5
27	6131	407.8	67	10400	394.0
28	6231	404.8	68	10500	392.7
29	6341	402.7	69	10600	391.4
30	6441	401.2	70	10700	390.2
31	6541	399.8	71	10800	389.4
32	6641	398.4	72	10900	388.6
33	6741	397.2	73	11000	387.9
34	6841	396.4	74	11200	387.3
35	6941	395.6	75	11400	386.4
36	7041	394.5	76	11600	385.4
37	7141	393.5	77	11700	384.8
38	7241	392.6	78	11800	384.0
39	7341	391.9	79	11910	383.0
40	7451	391.3	80	12010	382.0

Table A-2. Containment Atmosphere Temperature (Concluded)

	TIME (SECONDS)	TEMPERATURE (K)
161	26380	384.3
162	26480	383.4
163	26580	382.6
164	26780	381.8
165	27090	381.1
166	27190	380.4
167	27390	379.6
168	27790	380.3
169	28500	379.7
170	29400	378.9
171	29600	378.3
172	29900	377.6
173	30100	376.9
174	30300	376.3
175	30600	375.6
176	31000	374.9
177	31510	374.3
178	32310	373.7
179	34010	373.1
180	35720	372.6
181	37020	372.1
182	38630	371.6
183	43340	371.1
184	864900	371.1

Table A-3. Mole Fraction Steam in the Containment Atmosphere

	TIME (SECONDS)	MOLE FRACTION STEAM		TIME (SECONDS)	MOLE FRACTION STEAM
1	0	0.5423	41	5011	0.3624
2	826	0.5384	42	5221	0.3596
3	1034	0.5331	43	5431	0.3575
4	1140	0.5301	44	6031	0.3600
5	1243	0.5270	45	6231	0.3623
6	1346	0.5238	46	6441	0.3654
7	1449	0.5204	47	6641	0.3684
8	1551	0.5169	48	6841	0.3726
9	1655	0.5132	49	6941	0.3753
10	1758	0.5094	50	7141	0.3780
11	1861	0.5054	51	7341	0.3800
12	1965	0.5011	52	7651	0.3857
13	2066	0.4967	53	8181	0.3886
14	2167	0.4906	54	8481	0.3915
15	2267	0.4838	55	8691	0.3935
16	2368	0.4767	56	8991	0.3885
17	2468	0.4699	57	9091	0.3852
18	2568	0.4632	58	9191	0.3816
19	2670	0.4566	59	9291	0.3776
20	2772	0.4502	60	9491	0.3737
21	2874	0.4442	61	9591	0.3685
22	2976	0.4387	62	9691	0.3641
23	3076	0.4332	63	9791	0.3693
24	3178	0.4275	64	9891	0.3806
25	3279	0.4218	65	9991	0.3917
26	3379	0.4162	66	10090	0.4014
27	3480	0.4107	67	10190	0.4090
28	3581	0.4053	68	10300	0.4139
29	3682	0.3999	69	10400	0.4186
30	3782	0.3947	70	10500	0.4219
31	3882	0.3917	71	10700	0.4243
32	3983	0.3879	72	11600	0.4211
33	4085	0.3832	73	11800	0.4166
34	4188	0.3792	74	11910	0.4134
35	4289	0.3763	75	12010	0.4096
36	4391	0.3738	76	12110	0.4053
37	4491	0.3715	77	12210	0.4008
38	4601	0.3694	78	12310	0.3963
39	4701	0.3670	79	12410	0.3919
40	4811	0.3651	80	12510	0.3875

Table A-3. Mole Fraction Steam in the Containment Atmosphere (Continued)

	TIME (SECONDS)	MOLE FRACTION STEAM		TIME (SECONDS)	MOLE FRACTION STEAM
81	12610	0.3832	121	16840	0.2628
82	12710	0.3787	122	16940	0.2605
83	12910	0.3739	123	17040	0.2582
84	13010	0.3683	124	17140	0.2559
85	13110	0.3638	125	17240	0.2537
86	13210	0.3594	126	17340	0.2515
87	13310	0.3554	127	17440	0.2493
88	13420	0.3516	128	17540	0.2472
89	13620	0.3479	129	17650	0.2450
90	13720	0.3436	130	17750	0.2429
91	13820	0.3396	131	17850	0.2409
92	13920	0.3360	132	17950	0.2389
93	14020	0.3325	133	18050	0.2370
94	14120	0.3293	134	18150	0.2351
95	14220	0.3258	135	18250	0.2335
96	14320	0.3226	136	18350	0.2318
97	14430	0.3194	137	18450	0.2300
98	14530	0.3163	138	18550	0.2283
99	14630	0.3133	139	18650	0.2269
100	14730	0.3235	140	18750	0.2253
101	14860	0.3184	141	18850	0.2237
102	14930	0.3146	142	18950	0.2223
103	15030	0.3115	143	19050	0.2209
104	15130	0.3085	144	19150	0.2197
105	15230	0.3057	145	19260	0.2185
106	15330	0.3029	146	19360	0.2171
107	15430	0.3000	147	19560	0.2153
108	15530	0.2971	148	19760	0.2139
109	15630	0.2943	149	19960	0.2125
110	15730	0.2914	150	20160	0.2112
111	15840	0.2886	151	20460	0.2099
112	15940	0.2858	152	20960	0.2088
113	16040	0.2831	153	21670	0.2077
114	16140	0.2806	154	22270	0.2065
115	16240	0.2779	155	22970	0.2054
116	16340	0.2753	156	23970	0.2065
117	16440	0.2728	157	24370	0.2080
118	16540	0.2704	158	24680	0.2094
119	16640	0.2678	159	24880	0.2106
120	16740	0.2654	160	25080	0.2118

Table A-3. Mole Fraction Steam in the Containment Atmosphere (Continued)

	TIME (SECONDS)	MOLE FRACTION STEAM		TIME (SECONDS)	MOLE FRACTION STEAM
161	25280	0.2131	201	31510	0.3597
162	25480	0.2144	202	31610	0.3576
163	25680	0.2157	203	31710	0.3555
164	25780	0.2174	204	31810	0.3535
165	25880	0.2337	205	31910	0.3515
166	25980	0.2593	206	32010	0.3497
167	26080	0.2868	207	32110	0.3478
168	26180	0.3067	208	32310	0.3444
169	26280	0.3205	209	32510	0.3413
170	26380	0.3302	210	32710	0.3385
171	26480	0.3377	211	32910	0.3359
172	26580	0.3442	212	33110	0.3336
173	26680	0.3506	213	33310	0.3315
174	26780	0.3568	214	33510	0.3297
175	26880	0.3633	215	33810	0.3274
176	26990	0.3693	216	34120	0.3255
177	27090	0.3712	217	34520	0.3237
178	27290	0.3733	218	35120	0.3220
179	27590	0.3781	219	35620	0.3203
180	27790	0.3833	220	36120	0.3186
181	27990	0.3878	221	36820	0.3169
182	28190	0.3913	222	37420	0.3152
183	28400	0.3935	223	38020	0.3136
184	28700	0.3969	224	42440	0.3152
185	29000	0.3991	225	43540	0.3168
186	29800	0.3970	226	44540	0.3184
187	30000	0.3944	227	45440	0.3200
188	30200	0.3906	228	46450	0.3217
189	30300	0.3883	229	47550	0.3235
190	30400	0.3860	230	48650	0.3252
191	30500	0.3835	231	49760	0.3270
192	30600	0.3811	232	50960	0.3287
193	30700	0.3787	233	52160	0.3304
194	30800	0.3762	234	53270	0.3322
195	30900	0.3737	235	54270	0.3340
196	31000	0.3713	236	55270	0.3357
197	31100	0.3689	237	56380	0.3374
198	31200	0.3665	238	57680	0.3391
199	31300	0.3642	239	59190	0.3408
200	31410	0.3619	240	60890	0.3426

Table A-3. Mole Fraction Steam in the Containment Atmosphere (Concluded)

	TIME (SECONDS)	MOLE FRACTION STEAM
241	62700	0.3444
242	64600	0.3462
243	66810	0.3480
244	69320	0.3498
245	72230	0.3516
246	75040	0.3534
247	78760	0.3552
248	83580	0.3570
249	86490	0.3578

Table A-4. Rate of Steam Condensation From the Containment Atmosphere

	TIME (SECONDS)	CONDENSATION (g/s)		TIME (SECONDS)	CONDENSATION (g/s)
1	0	8302	41	4701	3677
2	521	8241	42	4811	3647
3	621	8137	43	5011	3710
4	725	8006	44	5111	3683
5	826	7889	45	5221	3990
6	930	7758	46	5321	3937
7	1034	7616	47	5431	3881
8	1140	7473	48	5531	3843
9	1243	7329	49	5631	4033
10	1346	7176	50	5731	4143
11	1449	7010	51	5831	4083
12	1551	6849	52	5931	3980
13	1655	6673	53	6031	3873
14	1758	6493	54	6131	3831
15	1861	6303	55	6341	3854
16	1965	6119	56	6441	3894
17	2066	5951	57	6541	3926
18	2167	5677	58	6641	3947
19	2267	5538	59	6741	3983
20	2368	5360	60	6841	4037
21	2468	5200	61	6941	4110
22	2568	5063	62	7241	4140
23	2670	4934	63	7451	4163
24	2772	4821	64	7651	7078
25	2874	4697	65	7761	5243
26	2976	4589	66	7861	4710
27	3076	4481	67	7971	4453
28	3178	4373	68	8081	4314
29	3279	4263	69	8181	4278
30	3379	4161	70	8581	4356
31	3480	4064	71	8791	4329
32	3581	3968	72	8891	4249
33	3682	3880	73	8991	4102
34	3882	5250	74	9091	3971
35	4085	4715	75	9191	3846
36	4188	4287	76	9291	3724
37	4289	4010	77	9391	6237
38	4391	3860	78	9491	4611
39	4491	3764	79	9591	4041
40	4601	3729	80	9691	3708

Table A-4. Rate of Steam Condensation From the Containment Atmosphere (Continued)

	TIME (SECONDS)	CONDENSATION (g/s)		TIME (SECONDS)	CONDENSATION (g/s)
81	9791	3867	121	14120	2576
82	9891	4255	122	14220	2487
83	9991	4750	123	14320	2437
84	10090	5266	124	14430	2392
85	10190	5613	125	14530	2350
86	10300	5641	126	14630	2307
87	10400	5694	127	14730	3945
88	10600	5599	128	14830	3011
89	10700	5488	129	14930	2503
90	10800	5417	130	15030	2232
91	10900	5344	131	15130	2075
92	11000	5290	132	15230	1980
93	11300	5240	133	15330	1920
94	11400	5176	134	15430	1876
95	11500	5103	135	15530	1845
96	11600	5016	136	15630	1818
97	11700	4911	137	15730	1794
98	11800	4772	138	15840	1772
99	11910	4603	139	15940	1750
100	12010	4420	140	16040	1729
101	12110	4238	141	16240	1699
102	12210	4095	142	16340	1670
103	12310	3973	143	16440	1660
104	12410	3865	144	16540	1647
105	12510	3761	145	16640	1610
106	12610	3733	146	16740	1598
107	12710	3629	147	16840	1558
108	12810	5895	148	16940	1538
109	12910	4493	149	17040	1520
110	13010	3921	150	17140	1501
111	13110	3599	151	17240	1479
112	13210	3344	152	17340	1454
113	13310	3195	153	17440	1432
114	13420	3086	154	17540	1408
115	13520	4245	155	17650	1386
116	13620	3552	156	17750	1361
117	13720	3171	157	17850	1338
118	13820	2907	158	17950	1313
119	13920	2759	159	18050	1291
120	14020	2655	160	18150	1267

Table A-4. Rate of Steam Condensation From the Containment Atmosphere (Continued)

	TIME (SECONDS)	CONDENSATION (g/s)		TIME (SECONDS)	CONDENSATION (g/s)
161	18250	1283	201	22770	1007
162	18350	1252	202	22870	1016
163	18450	1221	203	22970	1007
164	18550	1193	204	23070	1014
165	18650	1204	205	23170	1024
166	18750	1173	206	23270	1014
167	18850	1148	207	23370	1026
168	18950	1157	208	23470	1017
169	19050	1125	209	23570	1027
170	19150	1117	210	23670	1021
171	19360	1082	211	23770	1033
172	19460	1068	212	23970	1042
173	19660	1055	213	24170	1052
174	19760	1068	214	24370	1065
175	19860	1041	215	24580	1081
176	20160	1019	216	24780	1098
177	20360	1013	217	24980	1116
178	20460	1024	218	25280	1135
179	20560	1014	219	25480	1159
180	20660	1029	220	25780	1201
181	20760	1019	221	25880	1520
182	20860	1032	222	25980	2180
183	20960	1022	223	26080	2895
184	21070	1037	224	26180	3492
185	21170	1026	225	26280	3855
186	21270	1041	226	26380	4035
187	21370	1033	227	26480	4123
188	21470	1043	228	26580	4185
189	21570	1030	229	26680	4258
190	21670	1037	230	26780	4339
191	21770	1023	231	26880	4442
192	21870	1036	232	26990	4544
193	21970	1023	233	27090	4421
194	22070	1030	234	27190	4288
195	22170	1018	235	27290	4169
196	22270	1024	236	27390	4083
197	22370	1013	237	27490	4033
198	22470	1020	238	27590	4109
199	22570	1009	239	27790	4217
200	22670	1017	240	27990	4284

Table A-4. Rate of Steam Condensation From the Containment Atmosphere (Continued)

	TIME (SECONDS)	CONDENSATION (g/s)		TIME (SECONDS)	CONDENSATION (g/s)
241	28400	4249	281	32910	2571
242	28500	4220	282	33010	2557
243	28700	4270	283	33110	2544
244	28900	4247	284	33310	2522
245	29300	4214	285	33510	2508
246	29400	4150	286	33910	2494
247	29500	4086	287	35720	2481
248	29600	4029	288	36120	2467
249	29700	3975	289	37020	2450
250	29800	3921	290	37320	2434
251	29900	3868	291	37620	2422
252	30000	3789	292	38330	2409
253	30100	3703	293	39230	2423
254	30200	3619	294	39730	2437
255	30300	3537	295	40230	2452
256	30400	3461	296	40730	2464
257	30500	3389	297	41330	2479
258	30600	3322	298	41830	2494
259	30700	3256	299	42340	2506
260	30800	3196	300	42840	2521
261	30900	3145	301	43340	2535
262	31000	3095	302	43740	2548
263	31100	3047	303	44240	2562
264	31200	3009	304	44740	2575
265	31300	2969	305	45240	2589
266	31410	2934	306	45740	2603
267	31510	2900	307	46250	2616
268	31610	2866	308	46850	2633
269	31710	2835	309	47350	2646
270	31810	2804	310	47950	2661
271	31910	2777	311	48550	2676
272	32010	2750	312	49150	2692
273	32110	2724	313	49760	2705
274	32210	2699	314	50260	2719
275	32310	2676	315	50860	2733
276	32410	2656	316	51560	2749
277	32510	2637	317	52260	2764
278	32610	2618	318	52860	2779
279	32710	2602	319	53370	2794
280	32810	2586	320	53870	2809

Table A-4. Rate of Steam Condensation From the Containment Atmosphere (Concluded)

	TIME (SECONDS)	CONDENSATION (g/s)
321	54470	2826
322	54970	2841
323	55570	2856
324	56180	2871
325	57080	2887
326	57880	2902
327	58780	2917
328	59690	2932
329	60590	2947
330	61490	2962
331	62500	2978
332	63500	2993
333	64500	3009
334	65710	3025
335	66910	3041
336	68320	3057
337	69820	3073
338	73340	3088
339	75140	3105
340	76950	3121
341	79160	3136
342	81570	3152
343	84380	3168
344	86490	3177

Table A-5. Rate of Heat Removal From the Containment Atmosphere

	TIME (SECONDS)	HEAT REMOVAL (J/s)		TIME (SECONDS)	HEAT REMOVAL (J/s)
1	0	2.0480E 07	41	4289	1.2900E 07
2	104	2.0750E 07	42	4391	1.2280E 07
3	206	2.0470E 07	43	4491	1.1900E 07
4	521	2.0340E 07	44	4601	1.1820E 07
5	621	2.0110E 07	45	4701	1.1600E 07
6	725	1.9800E 07	46	4811	1.1720E 07
7	826	1.9520E 07	47	4911	1.1530E 07
8	930	1.9170E 07	48	5011	1.1740E 07
9	1034	1.8860E 07	49	5111	1.2940E 07
10	1140	1.8520E 07	50	5221	1.3510E 07
11	1243	1.8190E 07	51	5321	1.3610E 07
12	1346	1.7850E 07	52	5431	1.3300E 07
13	1449	1.7450E 07	53	5631	1.4490E 07
14	1551	1.7100E 07	54	5731	1.5190E 07
15	1655	1.6660E 07	55	5831	1.4980E 07
16	1758	1.6220E 07	56	5931	1.4470E 07
17	1861	1.5750E 07	57	6031	1.3730E 07
18	1965	1.5310E 07	58	6131	1.3270E 07
19	2066	1.4910E 07	59	6231	1.2990E 07
20	2167	1.4220E 07	60	6341	1.2860E 07
21	2267	1.3930E 07	61	6541	1.2760E 07
22	2368	1.3530E 07	62	6641	1.2690E 07
23	2468	1.3180E 07	63	6941	1.3170E 07
24	2568	1.2880E 07	64	7041	1.2790E 07
25	2670	1.2590E 07	65	7241	1.2670E 07
26	2772	1.2380E 07	66	7341	1.2530E 07
27	2874	1.2120E 07	67	7451	1.2660E 07
28	2976	1.1880E 07	68	7651	2.6880E 07
29	3076	1.1660E 07	69	7761	1.8730E 07
30	3178	1.1410E 07	70	7861	1.6090E 07
31	3279	1.1190E 07	71	7971	1.4520E 07
32	3379	1.0940E 07	72	8081	1.3690E 07
33	3480	1.0760E 07	73	8181	1.3390E 07
34	3581	1.0540E 07	74	8281	1.3250E 07
35	3682	1.0380E 07	75	8381	1.3090E 07
36	3782	1.0440E 07	76	8791	1.2780E 07
37	3882	1.6270E 07	77	8891	1.2600E 07
38	3983	1.7560E 07	78	8991	1.2110E 07
39	4085	1.5720E 07	79	9091	1.1690E 07
40	4188	1.4030E 07	80	9191	1.1300E 07

Table A-5. Rate of Heat Removal From the Containment Atmosphere (Continued)

	TIME (SECONDS)	HEAT REMOVAL (J/s)		TIME (SECONDS)	HEAT REMOVAL (J/s)
81	9291	1.0890E 07	121	13820	1.0200E 07
82	9391	2.3860E 07	122	13920	9.4940E 06
83	9491	1.6430E 07	123	14020	8.9950E 06
84	9591	1.3950E 07	124	14120	8.6360E 06
85	9691	1.2500E 07	125	14220	8.2710E 06
86	9791	1.2880E 07	126	14320	8.0850E 06
87	9891	1.3720E 07	127	14430	7.9370E 06
88	9991	1.4850E 07	128	14530	7.8140E 06
89	10090	1.5990E 07	129	14630	7.6890E 06
90	10190	1.6610E 07	130	14730	2.0880E 07
91	10300	1.6430E 07	131	14830	1.4660E 07
92	10500	1.6130E 07	132	14930	1.1360E 07
93	10600	1.5880E 07	133	15030	9.5410E 06
94	10700	1.5500E 07	134	15130	8.4470E 06
95	10800	1.5190E 07	135	15230	7.7580E 06
96	11000	1.4820E 07	136	15330	7.5160E 06
97	11300	1.4610E 07	137	15430	7.2010E 06
98	11400	1.4420E 07	138	15530	6.9780E 06
99	11500	1.4210E 07	139	15630	6.8050E 06
100	11600	1.3970E 07	140	15730	6.6730E 06
101	11700	1.3680E 07	141	15840	6.5630E 06
102	11800	1.3300E 07	142	15940	6.4690E 06
103	11910	1.3030E 07	143	16040	6.3860E 06
104	12010	1.2340E 07	144	16140	6.4300E 06
105	12110	1.1980E 07	145	16240	6.3340E 06
106	12210	1.1600E 07	146	16340	6.2340E 06
107	12310	1.1280E 07	147	16640	6.1400E 06
108	12410	1.1000E 07	148	16840	6.0210E 06
109	12510	1.0740E 07	149	17040	5.9880E 06
110	12710	1.0470E 07	150	17240	5.9270E 06
111	12810	2.1090E 07	151	17340	5.8700E 06
112	12910	1.5480E 07	152	17440	5.8290E 06
113	13010	1.3030E 07	153	17540	5.7890E 06
114	13110	1.1730E 07	154	17650	5.7540E 06
115	13210	1.0700E 07	155	17750	5.7010E 06
116	13310	1.0130E 07	156	17850	5.6590E 06
117	13420	9.7270E 06	157	17950	5.6060E 06
118	13520	1.6850E 07	158	18050	5.5580E 06
119	13620	1.3340E 07	159	18150	5.5030E 06
120	13720	1.1480E 07	160	18250	5.6520E 06

Table A-5. Rate of Heat Removal From the Containment Atmosphere (Continued)

	TIME (SECONDS)	HEAT REMOVAL (J/s)		TIME (SECONDS)	HEAT REMOVAL (J/s)
161	18350	5.5890E 06	201	22670	4.9200E 06
162	18450	5.4900E 06	202	22770	4.8530E 06
163	18550	5.3960E 06	203	22870	4.9140E 06
164	18650	5.5410E 06	204	22970	4.8520E 06
165	18750	5.4340E 06	205	23070	4.9010E 06
166	18850	5.3500E 06	206	23170	4.9440E 06
167	18950	5.4700E 06	207	23270	4.8920E 06
168	19050	5.3640E 06	208	23370	4.9560E 06
169	19260	5.3960E 06	209	23470	4.8930E 06
170	19360	5.2730E 06	210	23570	4.9530E 06
171	19460	5.2190E 06	211	23670	4.8980E 06
172	19560	5.2630E 06	212	23770	4.9630E 06
173	19660	5.1930E 06	213	23870	4.9120E 06
174	19760	5.2740E 06	214	23970	4.9860E 06
175	19860	5.1350E 06	215	24070	4.9380E 06
176	20160	5.0070E 06	216	24170	5.0040E 06
177	20260	5.0430E 06	217	24270	4.9570E 06
178	20360	4.9600E 06	218	24370	5.0360E 06
179	20460	5.0110E 06	219	24480	4.9960E 06
180	20560	4.9450E 06	220	24580	5.0790E 06
181	20660	5.0080E 06	221	24680	5.0360E 06
182	20760	4.9530E 06	222	24780	5.1220E 06
183	20860	4.9980E 06	223	24880	5.0790E 06
184	20960	4.9530E 06	224	24980	5.1600E 06
185	21070	5.0050E 06	225	25080	5.1270E 06
186	21170	4.9560E 06	226	25180	5.0980E 06
187	21270	5.0160E 06	227	25280	5.1900E 06
188	21370	4.9720E 06	228	25380	5.1570E 06
189	21470	5.0160E 06	229	25480	5.2440E 06
190	21570	4.9560E 06	230	25680	5.1910E 06
191	21670	4.9860E 06	231	25780	5.3620E 06
192	21770	4.9250E 06	232	25880	6.4230E 06
193	21870	4.9890E 06	233	25980	8.4250E 06
194	21970	4.9250E 06	234	26080	1.0340E 07
195	22070	4.9660E 06	235	26180	1.1700E 07
196	22170	4.9020E 06	236	26280	1.2410E 07
197	22270	4.9480E 06	237	26380	1.2670E 07
198	22370	4.8800E 06	238	26580	1.2760E 07
199	22470	4.9310E 06	239	26680	1.2830E 07
200	22570	4.8630E 06	240	26780	1.2950E 07

Table A-5. Rate of Heat Removal From the Containment Atmosphere (Continued)

	TIME (SECONDS)	HEAT REMOVAL (J/s)		TIME (SECONDS)	HEAT REMOVAL (J/s)
241	26880	1.3140E 07	281	31710	8.5420E 06
242	26990	1.3340E 07	282	31810	8.4750E 06
243	27090	1.2940E 07	283	31910	8.4150E 06
244	27190	1.2530E 07	284	32010	8.3560E 06
245	27290	1.2170E 07	285	32110	8.2990E 06
246	27390	1.1910E 07	286	32210	8.2480E 06
247	27490	1.1760E 07	287	32310	8.2000E 06
248	27590	1.1960E 07	288	32410	8.1590E 06
249	27790	1.2220E 07	289	32610	8.0820E 06
250	27890	1.2150E 07	290	32810	8.0210E 06
251	27990	1.2350E 07	291	33010	7.9650E 06
252	28290	1.2270E 07	292	33210	7.9200E 06
253	28400	1.2170E 07	293	33510	7.8790E 06
254	28500	1.2070E 07	294	35920	7.8330E 06
255	28700	1.2190E 07	295	36920	7.7890E 06
256	28900	1.2100E 07	296	37220	7.7460E 06
257	29200	1.2020E 07	297	37620	7.7000E 06
258	29400	1.1790E 07	298	39930	7.7410E 06
259	29500	1.1610E 07	299	40730	7.7830E 06
260	29600	1.1460E 07	300	41530	7.8220E 06
261	29700	1.1320E 07	301	42340	7.8630E 06
262	29800	1.1170E 07	302	43040	7.9030E 06
263	29900	1.1030E 07	303	43740	7.9430E 06
264	30000	1.0830E 07	304	44540	7.9840E 06
265	30100	1.0600E 07	305	45340	8.0270E 06
266	30200	1.0390E 07	306	46250	8.0700E 06
267	30300	1.0180E 07	307	47050	8.1110E 06
268	30400	9.9980E 06	308	47850	8.1540E 06
269	30500	9.8230E 06	309	48750	8.1960E 06
270	30600	9.6610E 06	310	49560	8.2380E 06
271	30700	9.5030E 06	311	50560	8.2860E 06
272	30800	9.3600E 06	312	51560	8.3290E 06
273	30900	9.2410E 06	313	52560	8.3730E 06
274	31000	9.1240E 06	314	53370	8.4180E 06
275	31100	9.0160E 06	315	54170	8.4630E 06
276	31200	8.9270E 06	316	54970	8.5080E 06
277	31300	8.8380E 06	317	55880	8.5530E 06
278	31410	8.7590E 06	318	57080	8.5960E 06
279	31510	8.6830E 06	319	58340	8.6400E 06
280	31610	8.6090E 06	320	59890	8.6840E 06

Table A-5. Rate of Heat Removal From the Containment Atmosphere (Concluded)

	TIME (SECONDS)	HEAT REMOVAL (J/s)
321	61290	8.7280E 06
322	62700	8.7720E 06
323	64200	8.8180E 06
324	66110	8.8640E 06
325	68020	8.9090E 06
326	70520	8.9560E 06
327	75950	9.0030E 06
328	79460	9.0490E 06
329	83580	9.0960E 06
330	86490	9.1140E 06

APPENDIX B. TABULATED UNCERTAINTY DISTRIBUTIONS

The tables in this appendix provide detailed uncertainty distributions calculated in this work for decontamination factors at 1800, 6480, 13680, 49680, and 86450 seconds as well as for the effective decontamination coefficients for the time intervals 0-1800, 1800-6480, 6480-13680, 13680-49680, 49680-86450 seconds. Uncertainty distributions were constructed at two levels of confidence—50 and 90 percent. The distributions are given as the range of values that characterize percentiles of the distribution at 5 percent intervals from 5 to 95 percent.

Table B-1. Uncertainty Distribution of the Decontamination Factor for Gap Release Material at 1800 Seconds

Percentile	Values of the Decontamination Factor Characteristic of the Indicated Percentile at a Confidence Level, C, of	
	C = 90%	C = 50%
5	1.180 to 1.185	1.181 to 1.183
10	1.183 to 1.192	1.185 to 1.192
15	1.190 to 1.195	1.192 to 1.194
20	1.192 to 1.197	1.194 to 1.196
25	1.195 to 1.199	1.196 to 1.198
30	1.197 to 1.201	1.198 to 1.199
35	1.198 to 1.202	1.199 to 1.202
40	1.200 to 1.204	1.201 to 1.203
45	1.202 to 1.204	1.203 to 1.204
50	1.203 to 1.205	1.204 to 1.205
55	1.204 to 1.207	1.2048 to 1.2054
60	1.205 to 1.210	1.205 to 1.207
65	1.206 to 1.212	1.207 to 1.210
70	1.206 to 1.212	1.210 to 1.213
75	1.207 to 1.215	1.213 to 1.215
80	1.214 to 1.221	1.215 to 1.217
85	1.216 to 1.227	1.219 to 1.224
90	1.222 to 1.229	1.225 to 1.228
95	1.228 to 1.233	1.229 to 1.232
	Mean = 1.2055	

Table B-2. Uncertainty Distribution of the Decontamination Factor for Gap Release Material at 6480 Seconds

Percentile	Values of the Decontamination Factor Characteristic of the Indicated Percentile at a Confidence Level, C, of	
	C = 90%	C = 50%
5	1.898 to 1.934	1.903 to 1.910
10	1.910 to 1.984	1.936 to 1.978
15	1.966 to 2.017	1.981 to 1.999
20	1.986 to 2.022	2.000 to 2.022
25	2.011 to 2.036	2.022 to 2.025
30	2.022 to 2.057	2.026 to 2.042
35	2.028 to 2.064	2.042 to 2.058
40	2.046 to 2.074	2.058 to 2.066
45	2.060 to 2.082	2.066 to 2.075
50	2.067 to 2.095	2.075 to 2.087
55	2.076 to 2.102	2.083 to 2.096
60	2.088 to 2.124	2.096 to 2.108
65	2.098 to 2.149	2.108 to 2.127
70	2.116 to 2.160	2.127 to 2.151
75	2.142 to 2.176	2.151 to 2.165
80	2.159 to 2.210	2.165 to 2.180
85	2.172 to 2.264	2.188 to 2.235
90	2.219 to 2.291	2.258 to 2.283
95	2.283 to 2.309	2.290 to 2.303
	Mean = 2.0921	

Table B-3. Uncertainty Distribution of the Decontamination Factor for Gap Release Material at 13680 Seconds

Percentile	Values of the Decontamination Factor Characteristic of the Indicated Percentile at a Confidence Level, C, of	
	C = 90%	C = 50%
5	3.905 to 4.222	3.926 to 4.118
10	4.108 to 4.412	4.222 to 4.345
15	4.308 to 4.493	4.388 to 4.424
20	4.415 to 4.652	4.439 to 4.548
25	4.475 to 4.683	4.556 to 4.672
30	4.582 to 4.766	4.672 to 4.702
35	4.673 to 4.902	4.702 to 4.835
40	4.706 to 5.084	4.805 to 4.947
45	4.840 to 5.218	4.908 to 5.128
50	4.979 to 5.293	5.100 to 5.241
55	5.156 to 5.413	5.220 to 5.300
60	5.260 to 5.628	5.295 to 5.440
65	5.317 to 5.734	5.420 to 5.654
70	5.482 to 5.935	5.651 to 5.829
75	5.694 to 6.115	5.830 to 6.006
80	5.870 to 6.518	6.045 to 6.245
85	6.107 to 6.860	6.402 to 6.623
90	6.580 to 7.328	6.814 to 7.191
95	7.213 to 8.147	7.326 to 7.582
	Mean = 5.3641	

Table B-4. Uncertainty Distribution of the Decontamination Factor for Gap Release Material at 49680 Seconds

Percentile	Values of the Decontamination Factor Characteristic of the Indicated Percentile at a Confidence Level, C, of	
	C = 90%	C = 50%
5	33.75 to 42.41	34.06 to 39.74
10	39.74 to 44.80	42.75 to 43.70
15	43.19 to 48.69	43.82 to 47.16
20	44.96 to 50.81	47.81 to 50.07
25	48.53 to 52.83	50.13 to 51.49
30	50.26 to 54.50	51.52 to 53.64
35	52.15 to 60.29	53.63 to 56.31
40	53.70 to 65.49	56.30 to 61.19
45	56.76 to 71.33	61.09 to 66.66
50	61.57 to 74.66	65.99 to 72.22
55	66.66 to 76.49	72.09 to 75.36
60	72.36 to 81.21	75.36 to 77.61
65	75.44 to 85.21	77.48 to 81.81
70	78.41 to 92.89	81.67 to 86.83
75	82.49 to 95.83	87.08 to 93.74
80	90.26 to 107.9	94.22 to 98.38
85	95.56 to 118.1	99.59 to 111.6
90	108.2 to 131.1	116.90 to 124.8
95	124.8 to 153.3	130.1 to 149.3
	Mean = 74.272	

Table B-5. Uncertainty Distribution of the Decontamination Factor for Gap Release Material at 86450 Seconds

Percentile	Values of the Decontamination Factor Characteristic of the Indicated Percentile at a Confidence Level, C, of	
	C = 90%	C = 50%
5	509.4 to 728.8	565.8 to 640.4
10	633.6 to 820.4	729.8 to 774.2
15	757.5 to 921.4	804.8 to 837.6
20	821.4 to 980.2	840.6 to 933.1
25	900.1 to 1029	933.1 to 992.3
30	951.0 to 1087	993.7 to 1062
35	1010 to 1165	1061 to 1117
40	1069 to 1418	1110 to 1278
45	1156 to 1554	1259 to 1465
50	1283 to 1622	1439 to 1568
55	1476 to 1746	1567 to 1651
60	1584 to 1897	1637 to 1748
65	1663 to 2145	1747 to 1964
70	1750 to 2319	1958 to 2198
75	1981 to 2560	2200 to 2394
80	2226 to 2673	2405 to 2604
85	2517 to 3118	2605 to 3002
90	2730 to 3816	3052 to 3488
95	3488 to 4515	3816 to 4011
	Mean = 1740	

Table B-6. Uncertainty Distribution of the Decontamination Factor for In-Vessel Release Material at 6480 Seconds

Percentile	Values of the Decontamination Factor Characteristic of the Indicated Percentile at a Confidence Level, C, of	
	C = 90%	C = 50%
5	1.218 to 1.228	1.220 to 1.222
10	1.222 to 1.240	1.229 to 1.235
15	1.232 to 1.244	1.237 to 1.242
20	1.241 to 1.245	1.242 to 1.245
25	1.243 to 1.249	1.245 to 1.247
30	1.245 to 1.254	1.247 to 1.250
35	1.248 to 1.258	1.250 to 1.255
40	1.251 to 1.260	1.255 to 1.258
45	1.255 to 1.260	1.258 to 1.260
50	1.258 to 1.263	1.260 to 1.261
55	1.260 to 1.266	1.261 to 1.264
60	1.261 to 1.270	1.264 to 1.268
65	1.265 to 1.275	1.267 to 1.272
70	1.268 to 1.277	1.272 to 1.276
75	1.273 to 1.279	1.276 to 1.279
80	1.276 to 1.285	1.277 to 1.279
85	1.278 to 1.297	1.282 to 1.291
90	1.286 to 1.302	1.296 to 1.301
95	1.301 to 1.305	1.302 to 1.304
	Mean = 1.2615	

Table B-7. Uncertainty Distribution of the Decontamination Factor for In-Vessel Release Material at 13680 Seconds

Percentile	Values of the Decontamination Factor Characteristic of the Indicated Percentile at a Confidence Level, C, of	
	C = 90%	C = 50%
5	2.496 to 2.640	2.515 to 2.587
10	2.583 to 2.719	2.642 to 2.700
15	2.674 to 2.766	2.717 to 2.741
20	2.720 to 2.831	2.742 to 2.786
25	2.759 to 2.859	2.797 to 2.843
30	2.822 to 2.896	2.844 to 2.863
35	2.848 to 2.995	2.860 to 2.913
40	2.876 to 3.096	2.908 to 3.026
45	2.914 to 3.142	3.022 to 3.098
50	3.033 to 3.177	3.096 to 3.145
55	3.117 to 3.216	3.145 to 3.191
60	3.156 to 3.327	3.183 to 3.258
65	3.191 to 3.370	3.255 to 3.341
70	3.267 to 3.440	3.338 to 3.390
75	3.343 to 3.663	3.394 to 3.484
80	3.413 to 3.928	3.511 to 3.716
85	3.626 to 4.101	3.727 to 3.983
90	3.976 to 4.295	4.004 to 4.207
95	4.217 to 4.772	4.294 to 4.450
	Mean = 3.227	

Table B-8. Uncertainty Distribution of the Decontamination Factor for In-Vessel Release Material at 49680 Seconds

Percentile	Values of the Decontamination Factor Characteristic of the Indicated Percentile at a Confidence Level, C, of	
	C = 90%	C = 50%
5	21.577 to 26.422	21.815 to 25.338
10	25.295 to 27.629	26.628 to 26.960
15	26.866 to 29.823	27.083 to 29.084
20	27.738 to 31.036	29.495 to 30.344
25	29.807 to 32.314	30.437 to 31.493
30	30.572 to 33.578	31.510 to 32.586
35	31.785 to 37.455	32.568 to 34.758
40	32.697 to 39.510	34.429 to 38.297
45	34.999 to 42.788	37.907 to 40.368
50	38.823 to 44.506	39.946 to 43.164
55	40.930 to 45.784	42.905 to 44.828
60	43.517 to 47.18[illegible]	44.624 to 46.174
65	45.351 to 50.696	46.087 to 48.688
70	46.407 to 54.269	48.408 to 51.000
75	49.028 to 57.028	51.025 to 54.615
80	53.052 to 64.887	54.813 to 58.212
85	56.456 to 71.613	59.169 to 67.024
90	65.171 to 77.349	67.065 to 73.026
95	73.277 to 88.873	76.970 to 86.498
	Mean = 44.461	

Table B-9. Uncertainty Distribution of the Decontamination Factor for In-Vessel Release Material at 86450 Seconds

Percentile	Values of the Decontamination Factor Characteristic of the Indicated Percentile at a Confidence Level, C, of	
	C = 90%	C = 50%
5	323.6 to 455.5	361.4 to 403.0
10	399.5 to 507.5	456.7 to 487.1
15	471.3 to 566.3	497.0 to 529.7
20	511.6 to 597.9	544.2 to 575.8
25	553.5 to 629.7	576.0 to 615.2
30	585.7 to 669.2	615.4 to 647.0
35	616.5 to 715.2	646.8 to 679.8
40	648.6 to 857.7	679.8 to 774.7
45	700.9 to 941.8	767.4 to 895.0
50	779.2 to 983.2	898.3 to 946.6
55	895.4 to 1040	946.1 to 989.6
60	946.8 to 1143	989.0 to 1045
65	995.2 to 1257	1041 to 1148
70	1054 to 1378	1147 to 1314
75	1164 to 1484	1316 to 1400
80	1363 to 1572	1410 to 1519
85	1475 to 1822	1534 to 1702
90	1600 to 2167	1738 to 2072
95	2072 to 2578	2167 to 2317
	Mean = 1034	

Table B-10. Uncertainty Distribution of Gap Release Effective Decontamination Coefficient, λ_e, Over the Period 0 – 1800 Seconds

Percentile	Values of Effective 6 (hr^{-1}) Characteristic of the Indicated Percentile at a Confidence Level, C, of	
	C = 90%	C = 50%
5	0.331 to 3.339	0.333 to 0.336
10	0.336 to 0.351	0.339 to 0.350
15	0.347 to 0.356	0.351 to 0.354
20	0.352 to 0.360	0.354 to 0.358
25	0.356 to 0.362	0.359 to 0.362
30	0.360 to 0.367	υ.362 to 0.363
35	0.362 to 0.368	0.363 to 0.367
40	0.364 to 0.371	0.367 to 0.369
45	0.367 to 0.372	0.369 to 0.371
50	0.369 to 0.373	0.371 to 0.373
55	0.371 to 0.376	0.373 to 0.374
60	0.373 to 0.381	0.373 to 0.376
65	0.374 to 0.384	0.376 to 0.382
70	0.377 to 0.390	0.382 to 0.386
75	0.384 to 0.391	0.386 to 0.390
80	0.388 to 0.400	0.390 to 0.393
85	0.390 to 0.409	0.396 to 0.404
90	0.402 to 0.413	0.406 to 0.411
95	0.411 to 0.418	0.413 to 0.417
	Mean = 0.3736 hr^{-1}	

Table B-11. Uncertainty Distribution of the Gap Release Effective Decontamination Coefficient, λ_e, Over the Period 1800 - 6480 Seconds

Percentile	Values of Effective 6 (hr^{-1}) Characteristic of the Indicated Percentile at a Confidence Level, C, of	
	C = 90%	C = 50%
5	0.365 to 0.377	0.367 to 0.368
10	0.368 to 0.392	0.378 to 0.390
15	0.385 to 0.401	0.391 to 0.396
20	0.393 to 0.403	0.398 to 0.402
25	0.399 to 0.408	0.402 to 0.404
30	0.403 to 0.413	0.404 to 0.409
35	0.405 to 0.417	0.409 to 0.414
40	0.410 to 0.419	0.414 to 0.417
45	0.415 to 0.422	0.417 to 0.420
50	0.417 to 0.424	0.419 to 0.422
55	0.420 to 0.429	0.422 to 0.425
60	0.423 to 0.434	0.425 to 0.430
65	0.426 to 0.440	0.430 to 0.435
70	0.431 to 0.444	0.435 to 0.441
75	0.438 to 0.447	0.441 to 0.444
80	0.442 to 0.456	0.444 to 0.449
85	0.446 to 0.471	0.450 to 0.464
90	0.458 to 0.479	0.470 to 0.477
95	0.477 to 0.483	0.478 to 0.482
	Mean = 0.4231 hr^{-1}	

Table B-12. Uncertainty Distribution of the In-Vessel Release Effective Decontamination Coefficient, λ_e, Over the Period 1800 – 6480 Seconds

Percentile	Values of Effective 6 (hr^{-1}) Characteristic of the Indicated Percentile at a Confidence Level, C, of	
	C = 90%	C = 50%
5	0.152 to 0.159	0.153 to 0.154
10	0.154 to 0.166	0.158 to 0.162
15	0.161 to 0.168	0.163 to 0.167
20	0.166 to 0.169	0.167 to 0.168
25	0.168 to 0.172	0.169 to 0.170
30	0.169 to 0.174	0.170 to 0.172
35	0.170 to 0.176	0.172 to 0.175
40	0.172 to 0.177	0.175 to 0.177
45	0.175 to 0.178	0.177 to 0.178
50	0.177 to 0.180	0.178 to 0.178
55	0.178 to 0.182	0.178 to 0.180
60	0.178 to 0.184	0.180 to 0.182
65	0.181 to 0.187	0.182 to 0.185
70	0.183 to 0.188	0.185 to 0.187
75	0.186 to 0.189	0.187 to 0.188
80	0.188 to 0.193	0.188 to 0.189
85	0.189 to 0.200	0.191 to 0.196
90	0.193 to 0.203	0.199 to 0.203
95	0.203 to 0.205	0.203 to 0.204
	Mean = 0.1785 hr^{-1}	

Table B-13. Uncertainty Distribution of the Effective Decontamination Coefficient, λ_e, Over the Period 6480 - 13680 Seconds

Percentile	Values of Effective 6 (hr^{-1}) Characteristic of the Indicated Percentile at a Confidence Level, C, of	
	C = 90%	C = 50%
5	0.358 to 0.379	0.360 to 0.372
10	0.371 to 0.390	0.379 to 0.388
15	0.384 to 0.397	0.390 to 0.393
20	0.391 to 0.407	0.394 to 0.403
25	0.397 to 0.410	0.404 to 0.408
30	0.406 to 0.417	0.409 to 0.412
35	0.409 to 0.428	0.412 to 0.419
40	0.413 to 0.441	0.419 to 0.433
45	0.419 to 0.452	0.432 to 0.446
50	0.434 to 0.461	0.443 to 0.455
55	0.446 to 0.468	0.454 to 0.462
60	0.457 to 0.474	0.462 to 0.469
65	0.463 to 0.487	0.469 to 0.476
70	0.471 to 0.505	0.476 to 0.491
75	0.484 to 0.521	0.491 to 0.508
80	0.497 to 0.555	0.511 to 0.539
85	0.520 to 0.585	0.543 to 0.575
90	0.566 to 0.604	0.576 to 0.588
95	0.591 to 0.658	0.604 to 0.633
	Mean = 0.4629 hr^{-1}	

Table B-15. Uncertainty Distribution of the Effective Decontamination Coefficient, λ_e, Over the Period 49680 - 86450 Seconds

Percentile	Values of Effective 6 (hr^{-1}) Characteristic of the Indicated Percentile at a Confidence Level, C, of	
	C = 90%	C = 50%
5	0.262 to 0.274	0.262 to 0.267
10	0.267 to 0.279	0.275 to 0.277
15	0.276 to 0.285	0.279 to 0.280
20	0.280 to 0.289	0.281 to 0.286
25	0.284 to 0.291	0.286 to 0.289
30	0.287 to 0.293	0.289 to 0.291
35	0.290 to 0.295	0.291 to 0.294
40	0.292 to 0.297	0.294 to 0.296
45	0.294 to 0.298	0.295 to 0.297
50	0.296 to 0.300	0.297 to 0.299
55	0.297 to 0.304	0.299 to 0.301
60	0.299 to 0.306	0.300 to 0.305
65	0.301 to 0.310	0.305 to 0.307
70	0.305 to 0.314	0.307 to 0.311
75	0.308 to 0.317	0.311 to 0.314
80	0.312 to 0.325	0.314 to 0.319
85	0.317 to 0.335	0.321 to 0.330
90	0.327 to 0.340	0.332 to 0.338
95	0.338 to 0.344	0.340 to 0.343
	Mean = 0.3007 hr^{-1}	